ANALYSIS OF THE EFFECTS OF PRE-PROCESSING AND DUAL-TASKING ON GAIT ACCELEROMETRY SIGNALS

by

Alexandre Millecamps

B.S. in Electrical Engineering, ESIGELEC, 2012

Submitted to the Graduate Faculty of

the Swanson School of Engineering in partial fulfillment

of the requirements for the degree of

Master of Science

University of Pittsburgh

2013

UNIVERSITY OF PITTSBURGH

SWANSON SCHOOL OF ENGINEERING

This thesis was presented

by

Alexandre Millecamps

It was defended on

November 22, 2013

and approved by

Ervin Sejdić, Ph. D., Assistant Professor, Department of Electrical and Computer

Engineering

Luis F. Chaparro, Ph. D., Associate Professor, Department of Electrical and Computer

Engineering

Ching-Chung Li, Ph. D., Professor, Department of Electrical and Computer Engineering

and Computer Science

Thesis Advisor: Ervin Sejdić, Ph. D., Assistant Professor, Department of Electrical and

Computer Engineering

ANALYSIS OF THE EFFECTS OF PRE-PROCESSING AND DUAL-TASKING ON GAIT ACCELEROMETRY SIGNALS

Alexandre Millecamps, M.S.

University of Pittsburgh, 2013

One-third of older adults over 65 years of age fall each year. Falls are the main cause of injury and death among this population. Understanding the causes of falling is therefore a necessity for gerontologists. Gait accelerometry is an important approach for the quantitative assessment of human walking. It is an inexpensive, portable and reliable method to measure trunk accelerations. The latter may give indications on balance control even though there is no agreed measure of it. Accelerometry requires the measured accelerations to be pre-processed, but previous studies have not studied thoroughly its effects on signal features. We therefore constituted a set of features in the time, frequency and time-frequency domains and we evaluated the impact of tilt correction and wavelet denoising – two pre-processing operations – on these features.

Signals used in this thesis were collected on 35 participants aged 65-year-old and over: 14 were healthy controls (HC), 10 had Parkinson's disease (PD) and 11 had peripheral neuropathy (PN). They walked on a treadmill at preferred speed. We first applied tilt correction and wavelet denoising separately, then we applied operations one after another. Denoising had nearly no effect on features compared to the raw accelerations. Tilt correction led to better discrimination between groups. Joint pre-processing operations showed trends that were similar to the tilt correction alone.

Older adults also face increasing difficulties to perform an activity during walking and this threatens their stability. Thus, during another trial, the same groups of subjects were asked to press a button at hearing a tone. We observed the impact of dual-tasking on the

features. Several features such as Lempel-Ziv complexity, bandwidth of accelerations and harmonic ratios remained unaffected by dual-task walking while the remaining features were affected. We also examined the impact of dual-tasking on each group. Task differences were almost the same for every group and revealed lower harmonic ratios during dual-task walking.

Keywords: Gait accelerometry, pre-processing effects, dual-task walking, signal features.

TABLE OF CONTENTS

LIST OF TABLES

LIST OF FIGURES

PREFACE

I would like to thank Dr. Mahmoud El Nokali, my advisor Dr. Ervin Sejdić and my family for their support. This work would not have been possible without them.

1.0   INTRODUCTION

1.1   HISTORY OF GAIT ANALYSIS: A BRIEF SUMMARY

The desire to analyze movement among living creatures dates back to Aristotle (384-322 BCE) who was already emitting hypotheses about their movements, but at that time, scientific reasoning was not accompanied with experimental proofs [1]. Much later, during the Renaissance (17th century), anatomists such as Giovanni Borelli (1608-1679), a student of Galileo Galilei (1564-1642), applied the latter's new scientific approach. Borelli was the first to perform experiments in gait analysis: he studied the muscle and tendon's biomechanics, but he made mistakes in the calculation of forces and he was unfortunately unable to use the mechanics theory of Newton (1642-1727) before he died [1]. In the 18th and 19th century, new ideas from several French physiologists were developed but were not followed by experiments. On the contrary, the German brothers Willhelm Eduard Weber (1804-1891) and Eduard Friedrich Weber (1806-1871) sustained their work with many experiments and published the book Mechanik der Gehwerkzeuge (Mechanics of the Human Walking Apparatus) in 1836 [1]. The development of photography began in the 20th century and was used by Etienne-Jules Marey (1830-1904) in France and Edward Muybridge (1830-1904) in the USA to perform gait analysis experiments on humans as well as animals [1, 2, 3, 4]. Nowadays the use of technology, such as video camera systems, to perform motion capture and accelerometry, coupled with computers to accelerate data processing, is common in gait analysis [2, 5, 6].

1.2 HUMAN LOCOMOTION

Humans start to walk when their center of mass falls outside the base of support [7] (Figure 1). One leg is moved after another to make a certain number of *steps.* Therefore the action of walking is cyclic, and its description can be done by focusing on one *stride* only. A stride is equivalent to two steps. For instance, the beginning of a stride can be taken at heel strike of one foot and ends at heel strike of the same foot. Since a stride corresponds to an entire walk cycle it is also called a *gait cycle.*
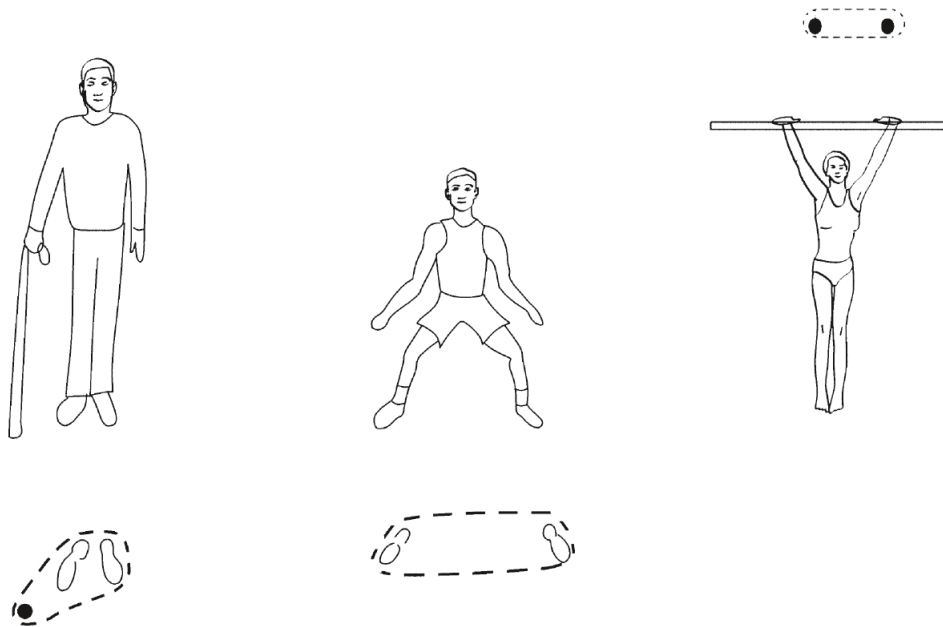
Figure 1: Base of support during various activities. Courtesy of [8].

As shown on Figure 2 the gait cycle can be described as follows [9]:

1. The cycle begins with heel contact of the right foot. The left foot is still in contact with the ground This is a *double support* phase and the beginning of the right stance phase. At this point, one relies on one leg only to maintain equilibrium.

2. The left foot leaves the ground. This is the end of the double support phase and the beginning of the left swing phase.

3. The left heel reaches the floor. This is the end of the left swing phase and the beginning of the left stance phase. The right foot is still on the ground, so it is also the beginning of a double support phase.

4. The right foot leaves the ground. This is the beginning of the right swing phase and the end of double support.

5. The right foot hits the ground. This is the beginning of a new gait cycle.

About 60% of the gait cycle corresponds to the stance phase while the remaining of the cycle corresponds to the swing phase. Also, the double support phases are characteristic of walking and do not appear during running [10].
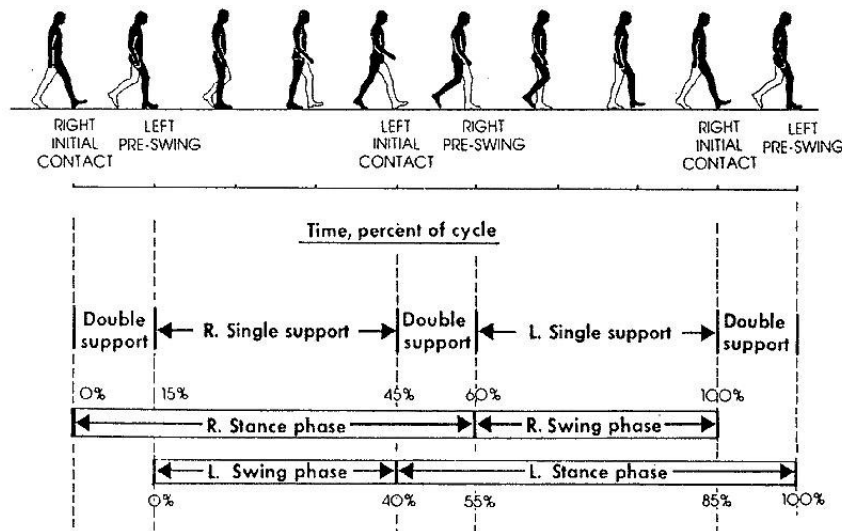
Figure 2: Gait cycle. Courtesy of http://atec.utdallas.edu/midori/Handouts/walkingGraphs.htm

This cycle is the result of complex interactions between three main sensory systems [7, 11, 12, 13]:

- *The vision system*: involved in motion planning and obstacle avoidance
- *The vestibular system*: senses linear and angular accelerations
- *The somatosensory system*: senses the position and velocity of all limbs, senses contact with the environment and senses orientation of gravity.

Impairment of one of these systems can be difficult to detect since one can compensate for a disability with another system. For instance, subjects with vestibular disorders compensate for them using their vision system: once they close their eyes, these subjects become unstable [7, 13].

1.3   MOTIVATIONS BEHIND GAIT ANALYSIS

Analyzing gait has clinical applications as a tool that helps physicians quantify, record and observe the evolution of gait of their patients and make decisions if a surgery is planned [2, 14, 5, 15, 16]. Gait impairments have various causes. They are often the result of neurological disorders due to age [17, 18] or diseases which include Parkinson's disease [19, 20, 21] and peripheral neuropathy [22, 23]. For physicians, an important fact to consider is that among the elderly population, more than one third of them fall each year and it is the main cause of morbidity and death among this population [24, 25, 26]. Understanding the dynamics of movement so as to predict falls and target treatments towards potential fallers is therefore of main importance [27, 28].

1.4   RESEARCH OBJECTIVES

The use of accelerometry was introduced as an inexpensive method to measure trunk accelerations with the advantage of providing the possibility to do it outside the laboratory

environment [29]. The purpose of this technique is to measure accelerations of the center of mass of a subject as it is known to be a indicator of motor control [7]. Many ways to quantify gait exist, but unfortunately no agreed measure of stability has been found.

Recently, studies have begun evaluating how dual-tasking impacts elderly people's balance control [30, 31]. Dual-task walking designates the performance of another activity during walking and it is performed on a daily basis (e.g. listening to music, looking at a phone or watching traffic during walking). In order to walk properly, elderly people require higher cognitive functions or more attention which may conflict with other tasks performed at the same time of walking and threaten their balance. Evaluating dual-tasking is therefore a necessity to understand the interaction between the various systems involved in balance control [30].

In our studies, we analyzed stride intervals and accelerations of the trunk from 35 subjects aged 65-year-old and over. Although several diseases affect gait we chose to focus particularly on Parkinson's disease and peripheral neuropathy which are at the origin of neurological disorders and are known to have an impact on gait. 14 subjects were healthy controls while 10 were suffering from Parkinson's disease and 11 had peripheral neuropathy.

In gait analysis, many characteristics can be used to characterize somebody's gait. Thus, we processed the acceleration signals and we constituted a set of features in the time domain, frequency domain and time-frequency domain with the purpose to answer several questions. We wanted first to understand what was the impact on pathologies on the features. Then we analyzed what were the effects of pre-processing on the features, since tilt correction and wavelet denoising are two operations that may be applied to the acceleration signals. Also, as dual-task walking happens frequently in every day life, we analyzed its effects on extracted features. Our results and future work are detailed in this thesis.

2.0   BACKGROUND

2.1   ASSESSING HUMAN GAIT

Gait analysis is useful when one wants to quantitatively measure the degree of stability of a subject. In order to do so, experiments are generally led during standing and walking.

2.1.1   Postural analysis

2.1.1.1   Using force platforms   Many studies have focused on postural analysis to assess balance control (e.g. [7, 32, 33, 34, 13, 35, 23]). In postural analysis, subjects are asked to stand on a force platform in order to measure the displacement of their *center of pressure* (COP). The COP is the point where the force that opposes gravity applies (Figure 3a). Thus, there is a COP under each foot and the position of the net COP is commonly used [7]. During standing, the net COP lies somewhere between the two legs depending on how much of the body weight each leg supports.

The idea behind the experiment is to use the COP as a indicator of equilibrium. Thus, by measuring the displacement of the COP, one could measure the extent of the sway of a subject [29]. Even if velocity, path length and frequency are features commonly used, no agreed characteristics of the COP displacement have been found [33].

Moreover it has been noted that there was a certain amount of confusion between the COP and the *center of mass* (COM) which is the point where the gravity force applies when the centers of mass of every limbs has been averaged. The COM should be used as an indicator of balance control [7]. It can be noted that the *center of gravity* (COG) is the projection of the COM on the ground. Using an inverted pendulum model of the human

6

body, the acceleration of the COM in the anterior-posterior and medio-lateral directions has been shown to be proportional to the difference between the COP and the COM, and this relationship can be used to estimate the position of the COM [36, 7]. Figure 3b shows that the COP moves around the COM with a higher amplitude. Therefore the position of the COM was also estimated using a low-pass filter on the COP data [37].

(a) During quiet standing

(b) Position of the COM and COP as a function of time
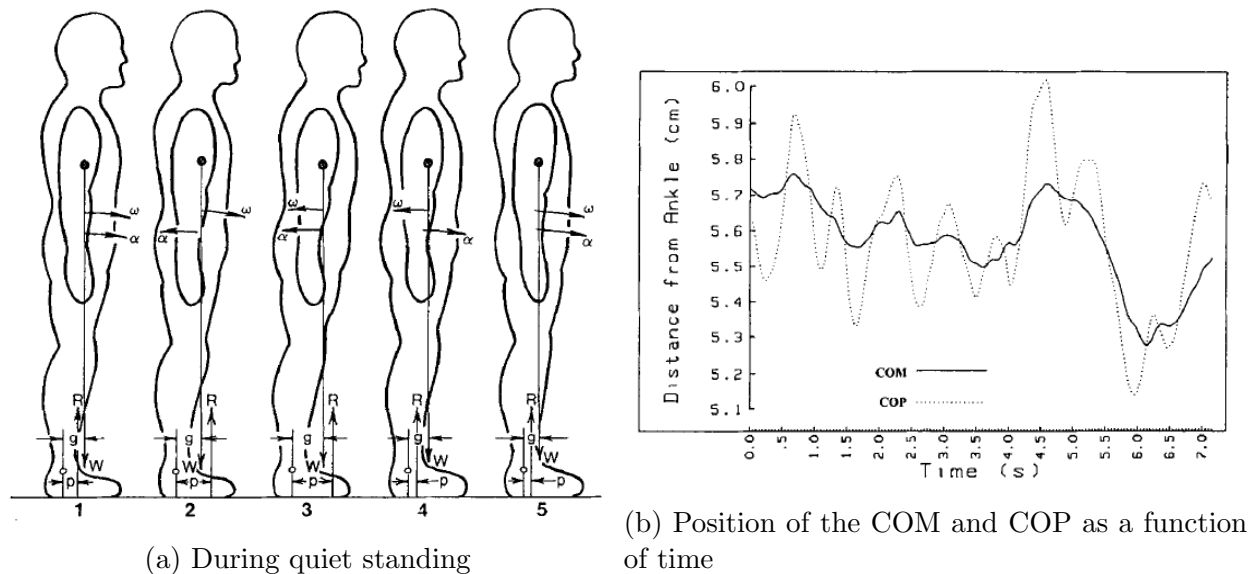
Figure 3: Positions of the COM and COP. Courtesy of [7]

Despite the fact that most falls occur during a form of locomotion [38, 39, 40], risks of falling have been evaluated during standing [17, 18, 41], which suggests that the mechanisms of stability involved during standing and locomotion are related. Using a state-space approach, evidence that it was not the case has been given [42]. Also, walking is a more challenging task. During standing, the central nervous system (CNS), which contains the brain and the spinal cord, has to maintain the COM in the base of support while during walking the COM lies outside the base of support and except during the phases of double support, balance is ensured by one limb only [7]. Thus, there is also a necessity to analyze gait during walking [43].

7

2.1.1.2 Using accelerometry The estimation of the COM's position from COP data was not precise enough [37] and other methods were needed to provide a better estimation. The position of the COM varies according to the subject, but its approximate position is known to be in the plane containing the L3 vertebra [44]. Therefore, placing an accelerometer in the lumbar region, at the L3 segment level (Figure 4), allows one to have a better estimation of the movements of the COM [33].
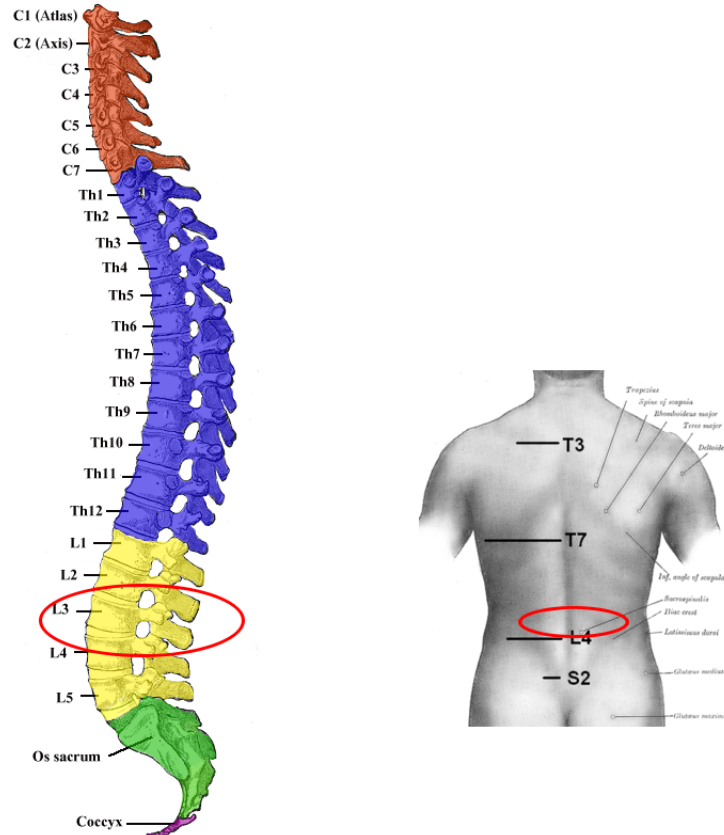
Figure 4: Position of the accelerometer. Adapted from http://en.wikipedia.org/wiki/Human_vertebral_column

A 3-axis accelerometer measures accelerations in three directions. Engineers generally denote them as $\overrightarrow{X}$, $\overrightarrow{Y}$ and $\overrightarrow{Z}$. However in medical terms (Figure 5), $\overrightarrow{X}$ is the medio-lateral direction (ML), $\overrightarrow{Y}$ is the vertical direction (V) and $\overrightarrow{Z}$ the anterior-posterior direction (AP).
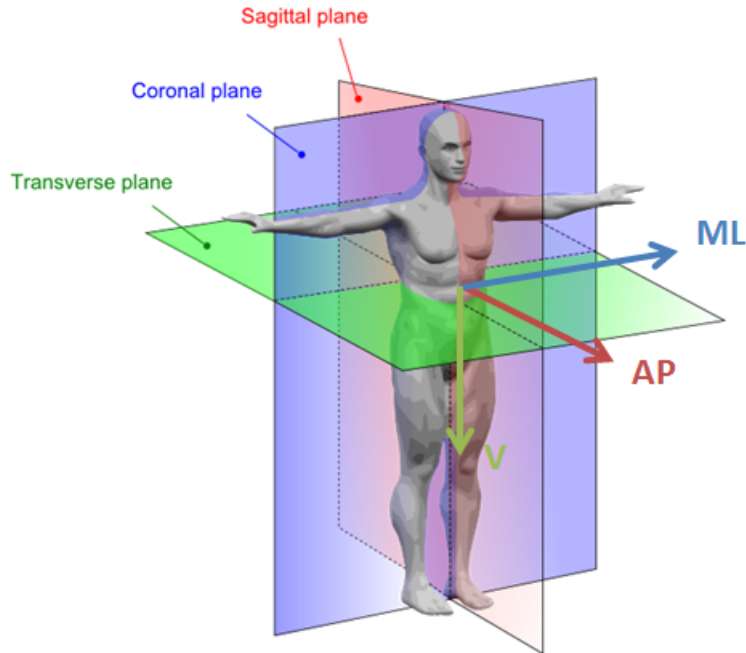
Figure 5: Anatomical planes and anatomical directions. Adapted from `http://commons.wikimedia.org/wiki/File:Human_anatomy_planes.svg`

The advantages of accelerometry are that it is precise, reliable and inexpensive [45]. Because the device is portable, experiments can also be lead in real-environment conditions so as to challenge gait in ways that would not be possible in a gait laboratory [29].

2.1.2 Dynamic gait analysis

When one observes the gait cycle, several ways to characterize gait easily come to mind. For instance, the *step length* and the *stride interval* are often used in studies. The step length is the distance between the heel of the leading leg to the heel of the trailing one while the stride interval is the time needed to perform a stride [9]. Identifying strides during an experiment is therefore a concern in dynamic gait analysis. Foot switches can be used to do so [46, 6, 28]. These are pressure sensors attached to the insoles in the shoes of a subject. However in our studies, they proved to be fragile thus motion capture was used to identify strides.

2.1.2.1 Using motion capture Motion capture systems [47, 48, 49, 50] are based on infrared cameras that track limbs' positions using markers placed on a subject near bone landmarks (Figure 6). Markers' positions are further processed to obtain movement information such as the angle between two limbs or the occurrence of strides using an algorithm [51]. Motion capture avoids wearing uncomfortable measurement devices. Markers can be placed on the trunk in order to measure its accelerations, but calculating accelerations of markers introduces errors since the markers' position data have to be derived twice. The placement of markers is not precise, either, since there may be an offset between the marker position and the bone landmark. It is, for example, impossible to point a marker exactly at the joint of two bones.
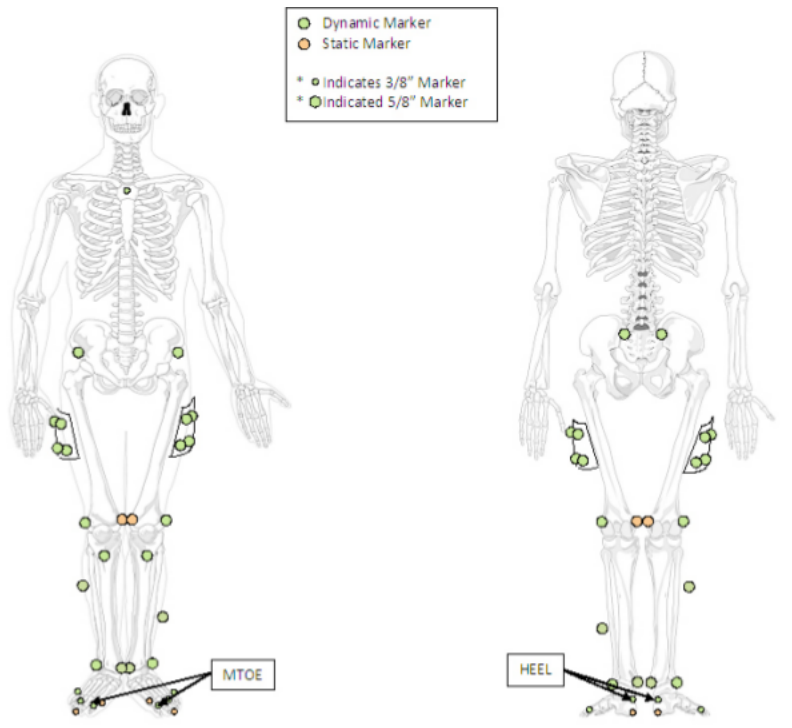
Figure 6: Positions of markers used in our studies

10

2.1.2.2   Using accelerometry   The method of accelerometry has been described in the previous section. Accelerometry can also be used to measure accelerations of the trunk during walking. Signals show periodic patterns which are related to the phases of the walk cycle [44, 43, 45].

The accelerations of the trunk in the vertical direction are biphasic i.e. they are periodic with two peaks per period. Each peak reaching 1.5 g correspond to a heel strike. The acceleration decreases to about 0.8 g after heel strike before it increases again in preparation of another heel strike. We notice here that the signal mean is 1 because the accelerometer also measures the gravity. Thus, mathematical procedures are necessary to correct measurements.

The accelerations in the AP direction are also biphasic and their amplitudes are smaller than those in the vertical direction. Before heel contact, the trunk accelerates backward to attain an acceleration of -0.5 g. Then the body accelerates forward reaching a peak of 0 g. Accelerations decrease again before the next heel strike.

Lastly, accelerations in the ML direction show a monophasic pattern. Peak accelerations can be seen after heel strike. However, accelerations in this anatomical direction have substantial variability between each period.
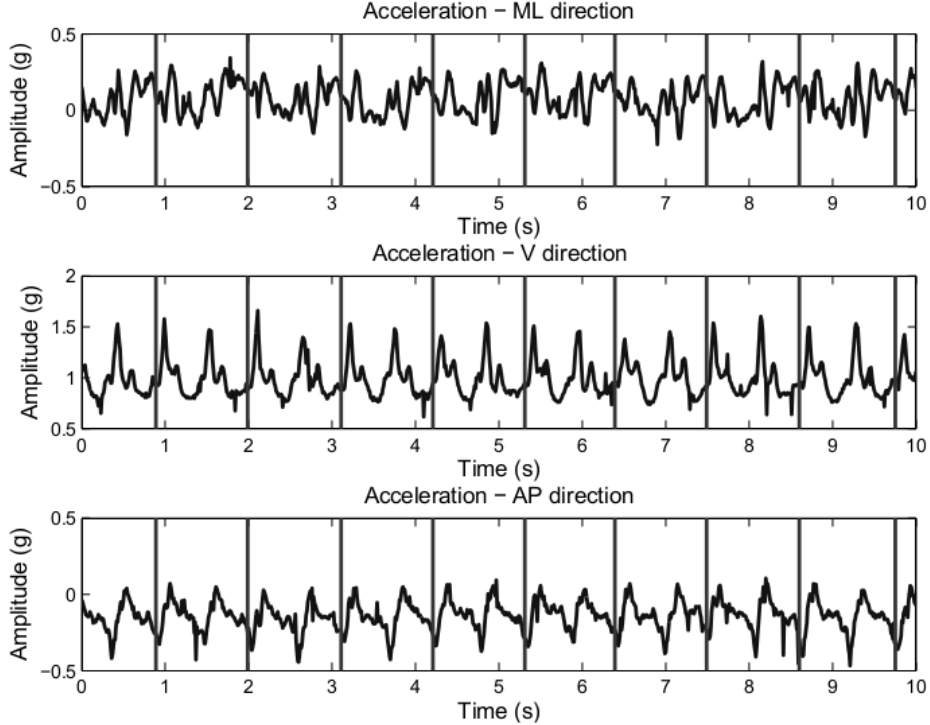
Figure 7: Raw accelerations in the ML, V and AP directions of a healthy subject. Vertical bars indicate heel strikes of the right foot

2.1.3 Processing of acceleration signals

2.1.3.1 Dynamic tilt correction In previous publications concerning gait analysis while walking [52, 53], it has been argued that a correction of the acceleration measurement is necessary due to the spine lordosis in the L3 region, the imprecise positioning of the accelerometer, and the effect of the gravity component over the measured accelerations. We performed tilt correction using the method developed by Moe-Nilssen [52]. Coordinates of the accelerometer were rotated to earth-vertical (Figure 8).

The accelerometer is situated near the L3 lumbar vertebra which minimizes the transverse plane offset rotation of the device. Therefore we assume that the AP acceleration is situated in the sagittal plane. θ_{AP} and θ_{ML} are the angles between the transverse plane and the measured accelerations. $\mathbf{a}_{H-AP}$ and $\mathbf{a}_{H-ML}$ are projections of the measured accelera-

12

tions in the new coordinate system. $\mathbf{a}_{V'}$ is the temporary corrected vertical acceleration i.e the acceleration after correcting the measured one in the AP plane and $\mathbf{a}_V$ is the vertical acceleration in the new coordinate system. Angles are positive above the horizontal axis and positive axes are horizontal to the right and vertical up.

The following equations operate the coordinate transform:

In the sagittal plane

$$\mathbf{a}_{H-AP} = \mathbf{a}_{AP}\cos(\theta_{AP}) - \mathbf{a}_v\sin(\theta_{AP}) \tag{2.1}$$

$$\mathbf{a}_{V'} = \mathbf{a}_{AP}\sin(\theta_{AP}) + \mathbf{a}_v\cos(\theta_{AP}) \tag{2.2}$$

In the coronal plane

$$\mathbf{a}_{H-ML} = \mathbf{a}_{ML}\cos(\theta_{ML}) - \mathbf{a}_{V'}\sin(\theta_{ML}) \tag{2.3}$$

$$\mathbf{a}_V = \mathbf{a}_{ML}\sin(\theta_{ML}) + \mathbf{a}_{V'}\cos(\theta_{ML}) - \mathbf{g} \tag{2.4}$$

where $\mathbf{g}$ is the gravity vector. Since the acceleration unit is g, we have $\mathbf{g} = 1$.

Moe-Nilssen [52] showed that the quantities $\sin(\theta_{AP})$ and $\sin(\theta_{ML})$ can be approximated by the mean of the accelerations in the AP and ML directions, respectively, for a large
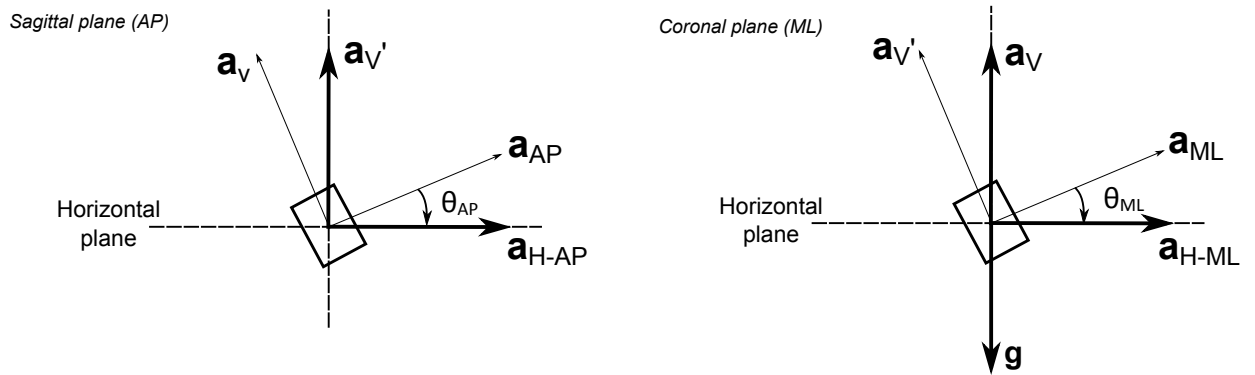
Figure 8: Acceleration vectors and their projection in the earth-vertical coordinate system: on the left accelerations in the sagittal plane; on the right accelerations in the coronal plane. $\mathbf{a}_{AP}$, $\mathbf{a}_{ML}$ and $\mathbf{a}_v$ denote the measured accelerations in the AP, ML and V directions respectively.

number of samples. The ith sample in the jth anatomical direction $\mathbf{a}_{i,j}$ (with $j = \{AP, ML\}$) can indeed be decomposed in two terms: one is the measured change of velocity $\mathbf{a}_{c(i,j)}$, the other is the static gravity component $\mathbf{a}_{g(i,j)}$:

$$\mathbf{a}_{(i,j)} = \mathbf{a}_{c(i,j)} + \mathbf{a}_{g(i,j)} \tag{2.5}$$

The expected value of the measured accelerations can be expressed as follows:

$$E[\mathbf{a}_{(i,j)}] = \lim_{n \to \infty} \frac{1}{n} \sum_{i=1}^{n} \mathbf{a}_{(i,j)} \approx \overline{\mathbf{a}}_j \tag{2.6}$$

Replacing the acceleration by the expression of a velocity change leads to the following expression:

$$E[\mathbf{a}_{c(i,j)}] = \lim_{n \to \infty} \frac{1}{n} \sum_{i=1}^{n} \mathbf{a}_{c(i,j)} = \lim_{n \to \infty} \frac{1}{n+1} \sum_{i=1}^{n+1} \frac{v_{(i,j)} - v_{(i-1,j)}}{\Delta t} = \lim_{n \to \infty} \frac{v_{(n+1,j)} - v_{(1,j)}}{(n+1)\Delta t} = 0 \tag{2.7}$$

where Δt denotes the sampling time. Assuming θ_j is constant we have:

$$E[\mathbf{a}_{g(i,j)}] = \lim_{n \to \infty} \frac{1}{n} \sum_{i=1}^{n} \mathbf{a}_{g(i,j)} = \mathbf{a}_{g(i,j)} \tag{2.8}$$

since the gravity vector is constant. Recalling equation 2.5, we have

$$E[\mathbf{a}_{(i,j)}] = E[\mathbf{a}_{c(i,j)}] + E[\mathbf{a}_{g(i,j)}] = E[\mathbf{a}_{g(i,j)}] \tag{2.9}$$

Hence

$$\overline{\mathbf{a}}_j = \mathbf{a}_{g(i,j)} \tag{2.10}$$

The gravity vector can be decomposed according to the measured accelerations:

$$\mathbf{g} = -\sin(\theta_{AP})\mathbf{a}_{AP} + \cos(\theta_{AP})\mathbf{a}_v \tag{2.11}$$

Finally, the approximation of the angles for a large number of samples is given by:

$$\overline{\mathbf{a}}_j = \sin(\theta_j) \tag{2.12}$$

Once these values are known, the estimated accelerations can be calculated. Figure 9 shows the results of tilt correction on acceleration signals measured on a healthy subject.
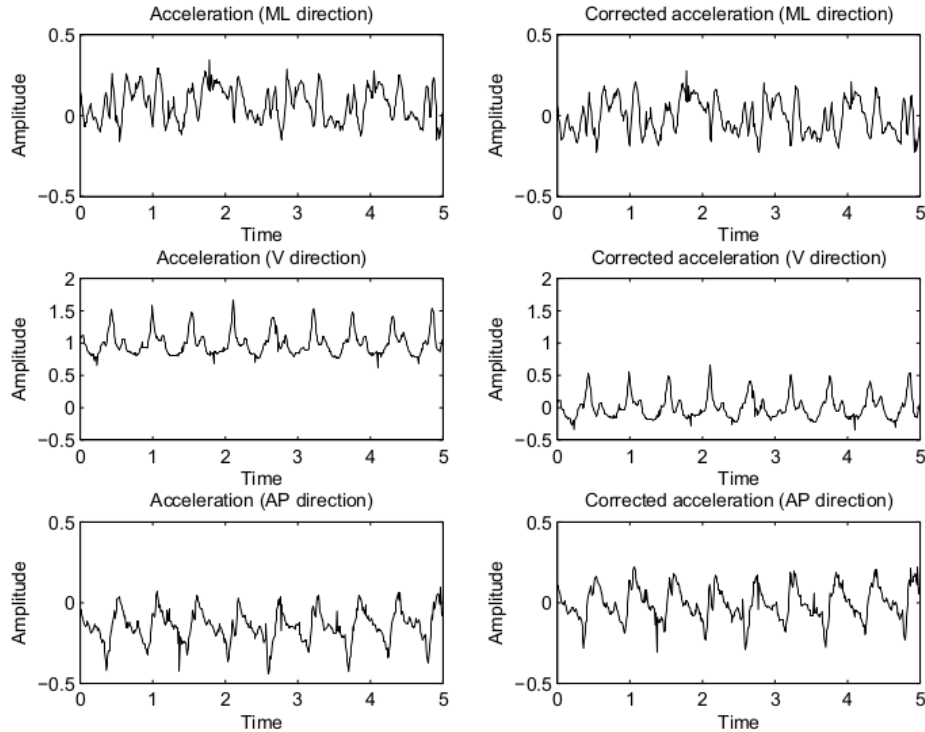
Figure 9: Comparison of signals before and after tilt correction for a HC control

2.1.3.2 Wavelet denoising Gait accelerometry signals can be corrupted by noise generated by the measurement device. A 10-level discrete wavelet transform using Meyer's discrete wavelet (Figure 10) and soft thresholding [54] can be applied to the data to denoise the signals. The wavelet analysis is a signal processing tool used to complement the Fourier analysis for understanding the non-stationary nature of many signals, especially biomedical signals (e.g., [55], [56], [57], [58], [59]).

Indeed the Fourier transform decomposes a signal in terms of complex exponential functions $e^{i\omega t}$ using the following formula:

$$\hat{f}(\omega) = \int_{-\infty}^{+\infty} f(t)e^{-i\omega t}dt \tag{2.13}$$

where f is a signal and $\hat{f}$ its Fourier transform.
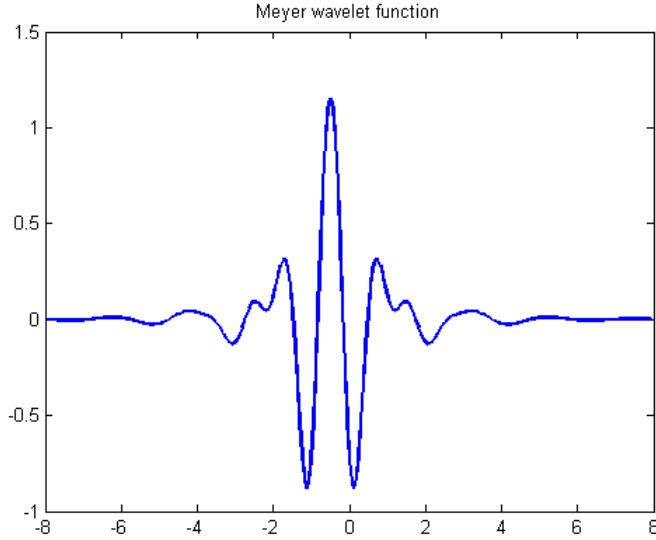
Figure 10: Meyer's mother wavelet

In wavelet theory, the complex exponential function is replaced by a function $\psi(t)$ called the *mother wavelet* having defined characteristics [60]:

$$\int_{-\infty}^{+\infty} |\psi(t)|dt = 0 \tag{2.14}$$

$$\int_{-\infty}^{+\infty} |\psi(t)|^2 dt < \infty \tag{2.15}$$

The first equation sets a zero-mean condition on the mother wavelet while the second one indicates it has finite energy. The mother wavelet is scaled and shifted, giving new wavelets which will be used to correlate the signal to analyze [60, 61]:

$$C_{u,s} = \int_{-\infty}^{+\infty} f(t)\psi_{u,s}^*(t)dt \tag{2.16}$$

where

$$\psi_{u,s}(t) = \frac{1}{\sqrt{s}}\psi(\frac{t-u}{s}) \tag{2.17}$$

The coefficients $C_{u,s}$ are the results of a continuous wavelet transform (CWT). However, the CWT implies an infinite number of dilatation and translation operations, which makes

it almost impractical in reality. Hence, there was a need for a method that would use a reduced number of dilatation and translation operations, while being able to obtain a good reconstruction of the original signal. In 1989, Mallat proposed an algorithm that implements a fast discrete wavelet transform by using a combination of high- and low-pass filters [62]. This technique is also known as sub-band coding in the signal processing community. Figure 11 describes how the algorithm was designed.
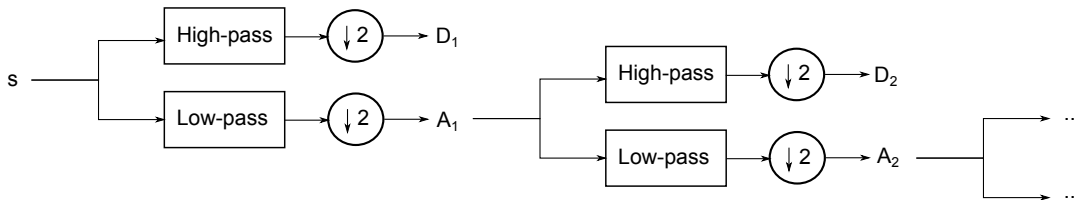
Figure 11: Fast wavelet transform algorithm: the signal s goes through a high-pass and a low-pass filter. The resulting signals are downsampled (one sample out of 2 is kept) so as to avoid data redundancy. The approximation signal A_1 and the detail signal D_1 are obtained. The n-level decomposition of the signal is computed by performing the same operation on the approximation signals obtained successively. The decomposition of the signal is given by the sequence $[A_n \, D_n \, D_{n-1} \, \ldots \, D_1]$.

Mallat's algorithm provides a signal representation in terms of the decomposition coefficients. These coefficients can be then manipulated to process the signal. Wavelet denoising is a signal operation consisting of applying a threshold on each signal coefficient [54], [63]. The threshold T is based on the 1st-level detail signal d_1 and was calculated as follows [57]:

$$T = \frac{med(|d1|)\sqrt{2\log n}}{0.6745}$$

where med is the median function and n is the length of the signal. The idea is that the coefficients associated with noise are below the threshold value, while the coefficients associated with the signal are above the threshold value. Thus, wavelet denoising is a more powerful tool compared to the classical low-pass filtering (e.g. using a Butterworth filter) as it enables the removal of noise from the whole frequency spectrum.

2.2 KNOWN GAIT CHARACTERISTICS OF CLINICAL POPULATIONS

Age and diseases have an impact on gait. Many studies have been carried out to determine gait characteristics of clinical populations.

2.2.1 Individuals with Parkinson's disease

Individuals with Parkinson's disease (PD) are known to walk with a stooped posture, make small shuffling steps and have difficulties initiating movements [21]. Because of this, it is expected that individuals with PD will have a less smooth walk than do controls [64]. Also, falls occur more frequently for PD subjects compared to controls: 1-year follow-up studies have shown that 70% of the subjects reported a fall during the study [19]. Postural sway in lateral directions is increased compared to age-matched controls [35] and fallers have increased stride-time variability [21].

2.2.2 Individuals with peripheral neuropathy

Peripheral neuropathy (PN) is a disease that affects nerves of the peripheral nervous system (PNS). The PNS is responsible for transmitting sensorimotor information to the brain. Symptoms of peripheral neuropathy include numbness or loss of sensitivity in the extremities. Individuals with PN have a higher risk of injuries during walking or standing [22]. Their gait is characterized by a lower walk speed, shorter steps and increased time spent in double support than their age-matched controls [65, 66]. PNs have an increased postural sway [23], their gait variability is increased, the smoothness of their walk is lower than controls and these effects increase in challenging environments [66].

3.0 METHODOLOGY

3.1 DATA ACQUISITION

A total of 35 patients aged 65 years old and older were enrolled in the experiment: 14 were healthy controls (HC), 10 had Parkinson's disease (PD) and 11 had peripheral neuropathy (PN). All of them could walk without human or mechanical assistance for at least 3 minutes. Details of participants have been reported in a previous study [67]. All subjects were assessed using a structured history and physical exam to ensure they met the general inclusion/exclusion criteria for the study. Potential subjects were excluded if they had any undiagnosed neurological (e.g. abnormal neurological examination such as spasticity, or severe paresis), musculoskeletal or cardiopulmonary conditions, or inadequate hearing or vision that would interfere with walking. Additionally, eligibility for HCs required no diagnosed neurological, vestibular or sensory disorders plus a biothesiometer reading at the malleolus < 20 v bilaterally. PDs had an established neurologist diagnosis of Parkinson's disease for at least one year according to the Hoehn and Yahr scale rating of 2 or 3, and a bioesthesiometer measure reading at the malleolus < 20 v bilaterally. Subjects were on a stable dosing schedule of Parkinson's medications for the prior three months. Subjects with PN had biothesiometer readings of ≥ 40 v bilateraly, indicating lose of vibratory sense. Subjects meeting the inclusion criteria completed the baseline assessments that included an overground walk used to determine self-selected treadmill speed.

Subjects meeting the inclusion/exclusion criteria walked on a computer-controlled treadmill (1.2 m wide by 2 m long). Safety was ensured by a harness system. An accelerometer was attached firmly to each patient over the L3 segment of the lumbar spine using a belt and a 4-inch wide elastic bandage wrapped over the accelerometer and the trunk (Figure 12). Linear accelerations were measured along the medial-lateral (ML), vertical (V) and anterior-posterior (AP) directions and sampled at 100 Hz.
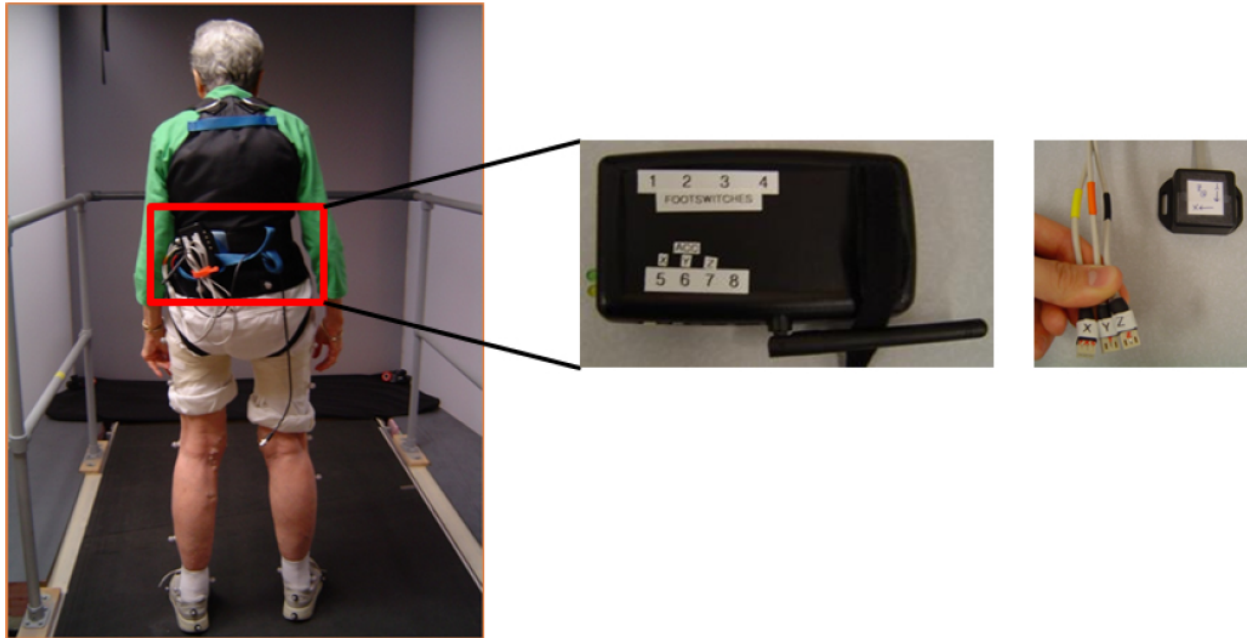
Figure 12: Experiement set up: a security harness, a 3-axis accelerometer and markers are placed on subjects

3.1.1 Tasks performed during the first study

After being accustomed to the instrumentation as well as walking on the treadmill, the subjects performed a 3-minute walk at a desired (usual) pace.

3.1.2 Tasks performed during the second study

After being accustomed to the instrumentation as well as walking on the treadmill, the subjects performed two walking trials. The first one, referred to as the normal task, consisted

of a 3-minute walk at a desired pace. The second trial, referred to as the dual task (DT), consisted of another 3-minute walk coupled with an auditory task. During this trial the subjects had to press a button in response to hearing a tone. The response time was measured before the trial while the patients remained seated. During the first 60 seconds of the second trial, the subjects walked at a desired pace (DT 1) and during the last two minutes they additionally performed the auditory task (DT 2).

3.2   DATA PRE-PROCESSING

3.2.1   Stride information retrieval

The algorithm developed by [51] was used to extract stride intervals from motion capture data.

3.2.2   Pre-processing in the first study

In the first study, we wanted to study the impact of pre-processing on the features we intended to extract. Therefore we applied tilt correction, wavelet denoising and a combination of these pre-processing operations, i.e. tilt correction then wavelet denoising, and wavelet denoising then tilt correction.

3.2.3 Pre-processing in the second study

In the second study, we applied tilt correction and wavelet denoising.

3.3   FEATURE EXTRACTION

In this section we describe the features we extracted from our signals.

3.3.1   Features common to both studies

3.3.1.1   Statistical features   A general form of signal can be defined as $X = \{x_1, x_2, \ldots, x_n\}$. Then, the following parameters can be extracted [68]:

- The standard deviation which characterizes the variability of signals was defined as follows:

$$\sigma_X = \sqrt{\frac{1}{n-1} \sum_{i=1}^{n} (x_i - \mu_X)^2} \tag{3.1}$$

  with μ_X being the mean of the signal.

- The skewness which characterizes the asymmetry of signals was defined as follows:

$$\xi_X = \frac{\frac{1}{n} \sum_{i=1}^{n} (x_i - \mu_X)^3}{\left(\frac{1}{n} \sum_{i=1}^{n} (x_i - \mu_X)^2\right)^{\frac{3}{2}}} \tag{3.2}$$

- The kurtosis which characterizes the behavior of extreme data points was defined as follows:

$$\gamma_X = \frac{\frac{1}{n} \sum_{i=1}^{n} (x_i - \mu_X)^4}{\left(\frac{1}{n} \sum_{i=1}^{n} (x_i - \mu_X)^2\right)^2} \tag{3.3}$$

- The cross-correlation coefficient at the zeroth lag defined as follows:

$$\eta_{XY} = \frac{\sum_{i=1}^{n} (x_i - \mu_X)(y_i - \mu_Y)}{\sqrt{\sum_{i=1}^{n} (x_i - \mu_X)^2} \sqrt{\sum_{i=1}^{n} (y_i - \mu_Y)^2}} \tag{3.4}$$

  with μ_X and μ_Y being the mean of signals X and Y.

3.3.1.2 Frequency features The following characteristics were identified in the frequency domain [69]:

- The peak frequency defined by:

$$f_p = \underset{f \in [0, f_{max}]}{\arg\max} |F_X(f)|^2 \tag{3.5}$$

where $F_X(f)$ is the Fourier transform of the signal and f_{max} is the sampling frequency (100 Hz in this experiment)

- The spectral centroid defined by:

$$f_c = \frac{\int_0^{f_{max}} f|F_X(f)|^2 df}{\int_0^{f_{max}} |F_X(f)|^2 df} \tag{3.6}$$

- The bandwidth defined by:

$$BW = \sqrt{\frac{\int_0^{f_{max}} (f - f_c)|F_X(f)|^2 df}{\int_0^{f_{max}} |F_X(f)|^2 df}} \tag{3.7}$$

- Calculating harmonic ratios is a way to assess smoothness of walking [70]. More recently, it has been suggested that harmonic ratios actually measure how symmetric a walk is [71]. Therefore we computed the harmonic ratios of low-pass filtered acceleration signals in every anatomical direction for each stride. The cutoff frequency of the filter was set to 30 Hz. First the discrete Fourier transform was calculated:

$$a_{stride} = \sum_{n=0}^{N-1} C_n \sin(n\omega_0 t + \phi_n) \tag{3.8}$$

where C_n is the harmonic coefficient, ω_0 is the stride frequency and ϕ_n is the phase. We then summed the first 20 harmonic coefficients to compute the harmonic ratios. The latter are defined as follows:

$$HR_{\text{AP and V}} = \left\langle \frac{\sum_{n=2,4,6,\ldots}^{20} C_n}{\sum_{n=1,3,5,\ldots}^{20} C_n} \right\rangle \tag{3.9}$$

$$HR_{\text{ML}} = \left\langle \frac{\sum_{n=1,3,5,\ldots}^{20} C_n}{\sum_{n=2,4,6,\ldots}^{20} C_n} \right\rangle \tag{3.10}$$

where $\langle \sum C_n / \sum C_n \rangle$ is the average ratio over all strides.

3.3.1.3 Time-frequency features We also took into account features in the time-frequency domain. A 10-level discrete wavelet transform was applied using discrete Meyer's wavelet [72]. The decomposition can be written as $W_X = [a_{10}\ d_{10}\ d_9 \ldots d_1]$ where a_{10} is the approximation signal and d_k is the kth-level detail signal.

- The relative energy in each wavelet decomposition level was computed as follows:

  The expression of the approximation signal energy is

  $$E_{a_{10}} = \|a_{10}\|^2 \tag{3.11}$$

  $\|\bullet\|$ being the Euclidean norm.

  The kth-level detail signal energy is expressed as follows:

  $$E_{d_k} = \|d_k\|^2 \tag{3.12}$$

  The total energy in the signal is:

  $$E_T = E_{a_{10}} + \sum_{k=1}^{10} E_{d_k} \tag{3.13}$$

  Finally the relative energy in each decomposition level is:

  $$\Phi_a = \frac{E_{a_{10}}}{E_T} \times 100\% \tag{3.14}$$

  $$\Phi_d = \frac{E_{d_k}}{E_T} \times 100\% \tag{3.15}$$

- Using the previously computed wavelet energy features, the wavelet entropy was calculated as follows:

  $$\Theta_X = -\Phi_{a_{10}} \log_2 \Phi_{a_{10}} - \sum_{k=1}^{10} \Phi_{d_k} \log_2 \Phi d_k \tag{3.16}$$

24

3.3.2 Additional features extracted in the second study

3.3.2.1 Stride-interval-based features The maximum Lyapunov exponent λ_L was calculated using the signal values $x(n)$ and forming the state-space representations [73]:

$$Z(n) = [x(n), x(n+T), \ldots, x(n+(d_E-1)T)] \tag{3.17}$$

where $Z(n)$ is the d_E-dimensional state vector, T is the time delay, and d_E is the embedding dimension. The time delay was estimated using the autocorrealtion function [74] and the embedding dimension was estimated using the method of false neighbors [75]. d_E was set to 5 as it was done in previous publications [76]. We estimated the maximum finite-time Lyapunov exponents using the formula

$$\ln(d_j(i)) \approx \lambda_L + \ln(D_j) \tag{3.18}$$

where $d_j(i)$ was the Euclidean distance between the jth pair of nearest neighbors after i discrete time steps and D is the initial average separation between neighboring trajectories [77]. The λ_L were estimated from the slopes of linear fits to curves defined by:

$$y(i) = \frac{1}{\Delta t} \langle \ln(d_j(i)) \rangle \tag{3.19}$$

where $\langle \ln(d_j(i)) \rangle$ represents the average over all values of j.

3.3.2.2 Information-theoretic features

- The Lempel-Ziv complexity (LZC) determines the predictability of a signal [78, 79, 80]. Accelerations signals were quantized then decomposed into k blocks. The normalized LZC was computed using the following expression [80]:

$$LZC = \frac{k \log_{100} n}{n} \tag{3.20}$$

Since the signal was quantized using 100 symbols we used a logarithmic base of 100. Large values of LZC indicate complex data.

- The entropy rate (ρ) measures the extent of regularity in a signal [81, 82]. The measure is particularly useful when a relationship among consecutive data points is anticipated. The first step is to to normalize X to zero mean and unit variance, by subtracting μ_X and dividing by σ_X. The normalized X was then quantized into 10 equally spaced levels represented by integers from 0 to 9, ranging from the minimum to maximum value. Using the quantized signal, $\hat{X} = \{\hat{x}_1, \hat{x}_2, \ldots, \hat{x}_n\}$, sequences of consecutive points in $\hat{X}$ of length L, $10 \leq L \leq 30$, were coded as a series of integers, $\Omega_L = \{w_1, w_2, \ldots, w_{n-L+1}\}$, according to the following:

$$w_i = 10^{L-1}\hat{x}_{i+L-1} + 10^{L-2}\hat{x}_{i+L-2} + \cdots + 10^0\hat{x}_i \tag{3.21}$$

This implies that w_i ranged from 0 to $10^L - 1$ and base 10 was used because there were 10 quantization levels. The Shannon entropy of L was defined as follows:

$$SE(L) = \sum_{j=0}^{10^L-1} p_{\Omega_L}(j) \ln p_{\Omega_L}(j) \tag{3.22}$$

where $p_{\Omega_L(j)}$ represents the probability of the value j in Ω_L, approximated by the corresponding sample frequency. The normalized entropy rate was then computed as follows:

$$NER(L) = \frac{SE(L) - SE(L-1) + SE(1)perc(L)}{SE(1)} \tag{3.23}$$

where $perc(L)$ is the percentage of the coded integers in Ω_L that occurred only once. Finally, an index of regularity, ρ, was calculated as the entropy rate feature in this study:

$$\rho = 1 - \min(NER(L)) \qquad (3.24)$$

which ranged from 0 (maximum randomness) to 1 (maximum regularity).

- Extending the entropy rate measure, the cross-entropy rate ($\Lambda_{X|Y}$) quantifies the entropy rate between two stochastic processes [82, 83]. This measure describes the predictability of a data point in one signal given a sequence of current and past data points in the other signal. First, both X and Y were normalized, quantized, and coded using the same methodology as for the entropy rate feature, yielding Ω_L^X and Ω_L^Y, respectively, with $10 \le L \le 30$. In addition, $\Omega_L^{X|Y}$ L was constructed as follows:

$$w_i^{X|Y} = 10^{L-1}\hat{x}_{i+L-1} + 10^{L-2}\hat{y}_{i+L-2} + \cdots + 10^0\hat{y}_i \qquad (3.25)$$

where $\hat{x}_i$ and $\hat{y}_i$ are the quantized samples of X and Y. Then, with $SE_X(L)$, $SE_Y(L)$, and $SE_{X/Y}(L)$ representing the Shannon entropies of Ω_L^X, Ω_L^Y, and $\Omega_L^{X|Y}$, respectively, the normalized cross-entropy of X given Y was computed as follows:

$$NCER_{X|Y}(L) = \frac{SE_{X|Y}(L) - SE_Y(L-1) + SE_X(1)perc_{X|Y}(L)}{SE_X(1)} \qquad (3.26)$$

where $perc_{X|Y}(L)$ is the percentage of the elements in $\Omega_L^{X|Y}$ that occurred only once. Next, the uncoupling function was defined as follows:

$$UF_{X,Y}(L) = \min(NCER_{X|Y}(L), NCER_{Y|X}(L)) \qquad (3.27)$$

Finally, the following index of synchronization was computed and utilized as the cross-entropy rate feature in this study:

$$\Lambda_{X|Y} = 1 - \min(UF_{X,Y}(L)) \qquad (3.28)$$

which ranged from 0 (X and Y are completely uncoupled) to 1 (perfect synchronization).

3.4   SUMMARY

Table 1 summarizes the content of our studies.

Table 1: Summary of tasks and signal processing performed in our studies

	Study 1	Study 2
Goal	What are the effects of pre-processing on features?	What are the effects of dual-tasking?
Tasks	Walk at self-selected speed during 3 min	Walk at self-selected speed during 3 min (Normal)
		Walk at self-selected speed during 1 min (DT 1)
		Walk + push button at hearing a tone during 2 min (DT 2)
Pre-processing	None	
	Tilt correction	
	Wavelet denoising	Tilt correction + Wavelet denoising
	Tilt correction + Wavelet denoising	
	Wavelet denoising + Tilt correction	
Extracted features	**Stride-interval-based features**	
	None	Maximum Lyapunov exponent λ_L
		Mean Stride Interval MSI
		Coefficient of variation CV
	Statistical features	
	Standard deviation σ	
	Skewness ξ	
	Kurtosis γ	
	Cross-correlation η	
	Information-theoretic features	
	None	Lempel-Ziv Complexity LZC
		Entropy rate ρ
		Index of synchronization Λ
	Frequency features	
	Peak frequency f_p	
	Spectral centroid f_c	
	Bandwidth BW	
	Harmonic ratio HR	
	Time-frequency features	
	Relative energy ϕ_a, ϕ_d	
	Wavelet entropy Θ	

4.0 RESULTS AND DISCUSSION

4.1 RESULTS FROM THE FIRST STUDY

The results of our analysis are summarized hereafter. Features are analyzed for each pre-proccesing operation and are compared to the original data.

4.1.1 Time and stride interval related features

Tables 2 and 3 summarize the differences found for the time domain features.

4.1.1.1 Original data We did not observe any differences between groups in any directions when considering the variability of signals σ ($p > 0.10$). When considering the skewness of signals, we found no statistical differences between groups along every direction ($p > 0.09$). Kurtosis values did not differ significantly for any group ($p > 0.29$) either. Finally, we found that $\eta_{ML,V}$ values were different between PD and PN subjects ($p < 0.02$). HC subjects also had greater harmonic ratios than PD subjects along every anatomical direction ($p < 0.03$).

Table 2: Group differences for features in the time domain. Legend - N.S: Not Significant; ×: no difference compared to raw data; △: HC vs. PN; ◇: HC vs. PD; □: PD vs. PN; +/-: feature added/removed compared to original data.

	Original	Corrected	Denoised	Corrected + denoised	Denoised + corrected
Standard deviation					
σ_{ML}	N.S.	×	×	×	×
σ_V	N.S.	×	×	×	×
σ_{AP}	N.S.	×	$+HC > PD$	×	×
Skewness					
ξ_{ML}	N.S.	$+PN > HC$	×	$+PN > HC$	$+PN > HC$
ξ_V	N.S.	×	×	×	×
ξ_{AP}	N.S.	×	×	$+HC > PD$	×
Kurtosis					
γ_{ML}	N.S.	×	×	×	×
γ_V	N.S.	×	×	×	×
γ_{AP}	N.S.	×	×	×	×
Cross-correlation					
$\eta_{ML,V}$	$PD > PN$	$-\square$	×	$-\square$	$-\square$
$\eta_{ML,AP}$	N.S.	×	×	×	×
$\eta_{V,AP}$	N.S.	×	×	×	×
Harmonic ratio					
HR_{ML}	$HC > PD$	×	$-\lozenge$	$-\lozenge$	$-\lozenge$
HR_V	$HC > PD$	$+PN > PD$	×	$+PN > PD$	$+PN > PD$
HR_{AP}	$HC > PD$	$+HC > PN$	×	$+HC > PN$	$+HC > PN$

Variability of signals statistically differed between anatomical directions for each group ($p < 0.01$). When we examined skewness of signals we found differences between every anatomical direction for each group ($p \ll 0.01$) except between ξ_{ML} and ξ_{AP} for PD subjects ($p > 0.26$). For HC patients, the behavior of extreme points was different between the ML and V directions ($p < 0.02$). Also, differences between $\eta_{ML,V}$ and $\eta_{V,AP}$ as well as between $\eta_{ML,AP}$ and $\eta_{V,AP}$ were identified for HC and PN subjects ($p \ll 0.01$). Each group had higher harmonic ratios in the V direction than in the ML direction ($p \ll 0.01$). Moreover, HCs and PNs had greater ratios in the AP direction than in the ML direction ($p \ll 0.01$). Finally, PN patients had a greater ratio in the V direction rather than in the AP direction ($p < 0.02$).

Table 3: Differences between anatomical directions for *statistical features*. For pre-processed data, only the differences with the original data are shown. Legend - N.S: Not Significant; ×: no difference compared to raw data; △: ML vs. V (ML,V vs. ML,AP for η); ◇: ML vs. AP (ML,V vs. V,AP for η); □: V vs. AP (ML,AP vs. V,AP for η); +/-: feature added/removed compared to original data

	Original			Corrected			Denoised			Corrected + denoised			Denoised + corrected		
	HC	PN	PD	HC	PN	PD	HC	PN	PD	HC	PN	PD	HC	PN	PD
σ *Standard deviation*	V > ML	V > ML		×	×	×	×	×		×	×	×	×	×	×
	AP > ML	AP > ML		×	-◇	-◇	×	×		×	-◇	-◇	×	-◇	-◇
	V > AP	V > AP		×	×	×	×	×		×	×	×	×	×	×
ξ *Skewness*	V > ML	V > ML	V > ML	×	×	×	×	×		×	×	×	×	×	×
	AP > ML	AP > ML	N.S.	×	-◇	×	×	×		×	-◇	×	×	-◇	×
	V > AP	V > AP	V > AP	×	×	×	×	×		×	×	×	×	×	×
γ *Kurtosis*	V > ML	N.S.	N.S.	-△	×		-△	×	×	-△	×	×	-△	×	×
	N.S.	N.S.	N.S.	×	×		×	+AP > ML	×	×	+AP > ML	+AP > ML	×	+AP > ML	×
	N.S.	N.S.	N.S.	×	×		×	×	×	×	+AP > V	+AP > V	×	+AP > V	×
η *Cross-correlation*	N.S.	N.S.	ML,V > ML,AP	×	×	-△		×		×	×	-△		×	-△
	V,AP > ML,V	V,AP > ML,V	V,AP > ML,V	×	×	×	×	×		×	×	×	×	×	×
	V,AP > ML,AP	V,AP > ML,AP	V,AP > ML,AP	×	×	×	×	×		×	×	×	×	×	×
HR *Harmonic ratio*	V > ML	V > ML	V > ML	×	×	×	×	×		×	×	×	×	×	×
	AP > ML	AP > ML	N.S.	×	-◇	×	×	×		×	-◇	×	×	-◇	×
	N.S.	V > AP	N.S.	+V > AP	×	+V > AP	+V > AP	×		+V > AP	×	+V > AP	+V > AP	×	+V > AP

31

4.1.1.2 Corrected data As shown in Figure 9, the correction shifted the signals to zero mean. The variability and kurtosis of signals followed the same trend as the uncorrected signals. Few changes between original and corrected data were noticed when analyzing asymmetry of signals (ξ feature). A difference between HC and PN participants was present in the corrected data along the ML axis ($p < 0.01$). Lastly, for $\eta_{ML,V}$ we did not find differences between PD and PN ($p > 0.92$). We also found that HCs had higher harmonic ratios than PNs in the AP direction ($p < 0.04$). Moreover the ratio along the V-axis was found higher for PNs than for PDs ($p < 0.04$).

The standard deviations of signals in the ML and AP directions were not different for PN and PD groups after correction ($p > 0.14$). We examined skewness of signals but did not find differences between the ML and AP directions for PN subjects ($p > 0.73$) anymore. The comparison of $\eta_{ML,V}$ and $\eta_{ML,AP}$ lead to no significant difference ($p > 0.68$). Lastly, the statistical difference for harmonic ratios between ML and AP disappeared for PN participants ($p > 0.15$). A new significant difference for HC controls and PD subjects was noticed: the ratio in the vertical direction was higher than in the anterior-posterior direction ($p < 0.01$).

4.1.1.3 Denoised data When considering the statistical features, we noticed a difference in standard deviations between HC and PD participants along the AP direction ($p < 0.05$) compared to the raw data. Skewness, kurtosis and cross-correlations followed the same trend as for the raw signals. For harmonic ratios, we found no difference between HC subjects and PD ones ($p > 0.10$) along the ML direction.

No changes in values for standard deviation, skewness and cross-correlation, and harmonic ratios could be noticed after denoising. The kurtosis difference between the ML and V directions did not appear anymore for HC patients ($p > 0.14$). For the PN group, γ_{AP} was different from γ_{ML} ($p < 0.05$).

4.1.1.4 Corrected and denoised data Skewness values were different between HCs and PNs ($p < 0.01$) along the ML-axis and between HCs and PDs along the AP-axis ($p < 0.05$). PD and PN groups were not significantly different for $\eta_{ML,V}$ values ($p > 0.70$). Harmonic ratios were not statistically different between HCs and PDs along the ML-axis

$(p > 0.1)$. We also found that HC controls had greater harmonic ratios than PN subjects in the AP direction $(p < 0.03)$. Moreover, PNs had a greater harmonic ratio than PDs in the vertical direction $(p < 0.05)$.

Our results showed that standard deviations were not statistically different in in the ML/AP directions for PN $(p > 0.56)$ nor for PD groups $(p > 0.45)$. No difference was observed for PN subjects when comparing ξ_{ML} and ξ_{AP} $(p > 0.81)$. The kurtosis of signals measured in all three directions were different for PNs $(p < 0.03)$ and PD subjects $(p < 0.05)$. No difference in kurtosis values could be observed between the V and ML directions for HC patients $(p > 0.24)$. Finally for PD patients, $\eta_{ML,V}$ and $\eta_{V,AP}$ were not statistically different $(p > 0.43)$. Harmonic ratios were not different between the ML and AP directions for PNs $(p > 0.51)$. We also observed that HC and PD subjects had a greater harmonic ratio in the vertical direction than in the anterior-posterior one $(p < 0.02)$.

4.1.1.5   Denoised and corrected data   The results were almost identical to the results obtained when performing tilt correction followed by denoising, except that skewness of signals measured along the ML-axis was different between HC and PN groups $(p < 0.01)$.

Similar results to tilt correction followed by denoising were obtained for this preprocessing step. However, no statistical differences between the values of $\eta_{ML,V}$ and $\eta_{ML,AP}$ were observed for PD subjects.

4.1.2   Frequency features

Tables 4 and 5 summarize the differences found for the frequency domain features.

4.1.2.1   Original data   No statistical differences for the peak frequencies were observed between groups $(p > 0.10)$. The spectral centroids exhibited differences between HC and PD subjects for signals acquired along the AP-axis $(p < 0.03)$. We finally noticed that signals measured on HC and PD subjects had different bandwidths in the ML and AP directions $(p < 0.03)$.

Table 4: Group differences for frequency features. Legend - N.S: Not Significant; $\times$: no difference compared to raw data; $\triangle$: HC vs. PN; $\Diamond$: HC vs. PD; $\square$: PD vs. PN; +/-: feature added/removed compared to original data

	Original	Corrected	Denoised	Corrected + denoised	Denoised + corrected
Peak frequency					
f_{pML}	N.S.	$+HC > PD$ $+HC > PN$	$\times$	$\times$	$\times$
f_{pV}	N.S.	$\times$	$\times$	$\times$	$\times$
f_{pAP}	N.S.	$\times$	$\times$	$\times$	$\times$
Centroid					
f_{cML}	N.S.	$\times$	$\times$	$\times$	$\times$
f_{cV}	N.S.	$\times$	$\times$	$\times$	$\times$
f_{cAP}	$PD > HC$	$+PN > HC$	$-\Diamond$	$+PN > HC$	$+PN > HC$
Bandwidth					
BW_{ML}	$PD > HC$	$\times$	$\times$	$\times$	$\times$
BW_{V}	N.S.	$\times$	$\times$	$\times$	$\times$
BW_{AP}	$PD > HC$	$+PN > HC$	$+PN > HC$	$+PN > HC$	$+PN > HC$

When we analyzed peak frequencies, we observed statistical differences for PNs and PDs between the ML and V directions and between the ML and AP directions ($p < 0.02$). The spectral centroids were statistically different between the ML and V directions for all groups ($p < 0.02$) and between the V and AP directions for PN and PD groups ($p \ll 0.01$). Finally, we observed differences for all groups between bandwidths of signals acquired along the V and AP directions ($p \ll 0.01$) as well as between the ML and V directions ($p \ll 0.01$).

4.1.2.2 Corrected data In the ML direction we found that signals retrieved from HC subjects had greater peak frequencies than PD ($p < 0.02$) and PN ($p < 0.03$) patients.

Table 5: Differences between anatomical directions for frequency features. For pre-processed data, only the differences with the original data are shown. Legend - N.S: Not Significant; ×: no differences compared to the original; △: ML vs. V (ML,V vs. ML,AP for η); ◇: ML vs. AP (ML,V vs. V,AP for η); □: V vs. AP (ML,AP vs. V,AP for η); +/-: feature added/removed compared to original data

	Original			Corrected			Denoised			Corrected + denoised			Denoised + corrected		
	HC	PN	PD	HC	PN	PD	HC	PN	PD	HC	PN	PD	HC	PN	PD
Peak frequency															
f_p	N.S.	$V > ML$			×	×		×	×	×	×	×	×	×	×
	N.S.	$AP > ML$			×	×		×	×	×	×	×	×	×	×
	N.S.	N.S.		$+AP > V$	×	×		×	×	×	×	$+V > AP$	×	×	×
Centroid															
f_c	$ML > V$	$ML > V$		×	×	×	$-\triangle$	$-\triangle$	$-\triangle$	×	$-\triangle$	$-\triangle$	×	$-\triangle$	$-\triangle$
	N.S.	N.S		$+AP > ML$	$+AP > ML$	×	×	$+AP > ML$	×	×	$+AP > ML$	×	×	$+AP > ML$	×
	N.S.	$AP > V$	$+AP > V$	×	×	×	×	×	×	×	×	×	×	×	×
Bandwidth															
BW	$ML > V$			×	×		$-\triangle$	×	×	×	×		×	×	
	N.S.			×	$+AP > ML$		×	$+AP > ML$	×	×	$+AP > ML$		×	$+AP > ML$	
	$AP > V$			×	×		×	×	×	×	×		×	×	

For spectral centroids, we observed a difference between PN and HC groups ($p < 0.04$) when looking at f_{cAP}. Lastly, BW_{AP} values were different for PN and HC volunteers ($p < 0.04$).

HC subjects had different spectral centroids when we compared signals along the AP-axis and V-axis ($p < 0.03$). For PNs, we also found that f_{cAP} was greater than f_{cML} ($p < 0.03$). Differences between bandwidths of signals in the AP and ML directions were found for PN ($p < 0.03$) and PD groups ($p < 0.05$).

4.1.2.3   Denoised data   No differences for f_{cAP} were found between HC and PD groups after denoising signals ($p > 0.05$). PN and HC groups had different bandwidths along the AP-axis ($p < 0.02$).

After denoising signals, we did not observe differences for any group between the ML and V directions when we analyzed spectral centroids ($p > 0.05$). However, we observed different centroid values between signals in the AP and ML directions for PN subjects ($p < 0.04$). Bandwidths for signals along the ML and V directions were not statistically different for HCs ($p > 0.06$). Signals from PN subjects had different bandwidth values in the AP and ML directions ($p < 0.04$).

4.1.2.4   Corrected and denoised   When comparing centroids for the corrected-denoised data and the raw data, we found that spectral centroids were different between PN and HC groups for signals measured in the AP direction ($p < 0.05$). The same trend could be observed for the bandwidth of these signals ($p < 0.01$).

We noticed that spectral centroids f_{cML} did not differ significantly from f_{cV} for PN ($p > 0.49$) and PD subjects ($p > 0.05$) after pre-processing signals. However, statistical differences between the ML and AP directions were observed for PN subjects only ($p < 0.02$). Bandwidths of signals in the AP and ML directions were different for PN and PD subjects ($p < 0.01$).

4.1.2.5   Denoised and corrected data   The same results were obtained as for performing tilt correction followed by denoising.

Significant differences were observed between peak frequencies of signals in the V and AP directions for PN subjects ($p \ll 0.01$). Otherwise the same trend as the corrected-denoised data was observed.

4.1.3   Time-frequency features

The four last detail level coefficients held nearly no energy. Thus, we did not consider these levels any further. Denoising did not affect the energy in the time-frequency bands. However applying correction changed the repartition of the energy. Indeed in the vertical direction the energy of the approximation signal decreased whereas the one in the 10$^{\text{th}}$ to the 5$^{\text{th}}$ detail signal increased. Depending on the decomposed signal studied differences between groups and anatomical directions were also observed. When both pre-processing operations were applied we could observe similar results to the ones we observed when applying correction only.

4.1.3.1   Original data   We did not observe significant groups differences in any time-frequency band for accelerations measured along the medio-lateral axis ($p > 0.06$). More than 99% of the energy of the V acceleration signals was concentrated in the approximation level. We discarded the rest of the coefficients in the V direction as the detail signals contained insignificant amounts of energy. However, no group differences could be seen along this axis ($p > 0.98$) or the AP axis ($p > 0.40$). No group differences were observed for the wavelet entropy of signals ($p > 0.17$).

For all groups, the a_{10} coefficients from the V direction contained higher energy than the same coefficients in the ML ($p \ll 0.01$) and AP direction ($p < 0.04$). Also, HCs had higher energy contained in a_{10} coefficients in the AP direction than in the ML direction ($p < 0.04$). d_8 coefficients contained higher energy in the ML direction than in the V direction for all groups ($p < 0.04$) and in comparison to the AP direction for the HC group ($p \ll 0.01$). Signals from PD subjects had higher energy in the AP direction compared to the signals in

the V direction ($p < 0.04$). In the 7$^{\text{th}}$ decomposition level, the energy was higher for signals retrieved along the ML-axis compared to those along the V direction ($p \ll 0.01$) and the AP direction ($p < 0.03$) for HC subjects. However no difference was noticed when we compared the signals in the V and AP directions ($p > 0.08$). In any direction, no differences were noticed for the other groups ($p > 0.2$). We noticed that the energy was lower for d_6 signals along the V-axis compared to those along the AP-axis for HCs ($p < 0.01$). For all groups, the energy in d_5 signals was higher along the ML-axis than the V-axis ($p < 0.04$). For PD subjects, we noticed that signals in the ML direction had higher energy compared to the AP direction ($p < 0.05$). We did not observed any difference when we compared signals in the V and AP directions ($p > 0.22$).

Interestingly we noticed that for each group the entropy values in the V direction were close to 0 while they were higher in the other directions ($p \ll 0.01$). We also noticed that Θ_{ML} was higher than Θ_{AP} for HCs ($p < 0.01$) and PD subjects ($p < 0.02$), while we observed no difference for PN subjects ($p > 0.1$).

4.1.3.2 Corrected data After the correction step, we noticed that the energy in wavelet decomposition levels was repartitioned for every group in every direction. HCs had higher energy than PD subjects along the ML-axis in the d_7 signal ($p \ll 0.01$). The same results were obtained for HCs and PNs when we analyzed the d_7 ($p < 0.02$) and d_5 ($p < 0.05$) detail signals along the same direction. In the V direction, while most of the energy was concentrated in the approximation signal for the raw data, the energy in the approximation signal after correction diminished and increased in the first 6 detail signals $\Phi_{V_{d_{10}}}, \Phi_{V_{d_9}}, \ldots, \Phi_{V_{d_5}}$ ($p \ll 0.01$). However, we did not notice any group differences along the V-axis. Statistical differences along the AP-axis were observed in the d_7 signals between HC and PD/PN subjects ($p < 0.02$) and in the d_6 detail signals between HCs and PNs ($p < 0.05$).

Overall the entropy in the V direction was lower than in the other directions. However for PN and PD subjects it was not statistically different from the entropy in the ML direction ($p > 0.19$) and from the entropy in the AP direction for PN patients ($p > 0.06$). Finally Θ_{ML} and Θ_{AP} were not statistically different for any group ($p > 0.28$).

After correction there were no significant differences between a_{10} signals in the V and ML direction and signals in the V and AP directions for all groups ($p > 0.05$). However, we observed that signals from PDs had higher energy in the ML direction than the AP direction ($p < 0.04$). The energy in the d_8 signals was not distinguishable between the ML and V directions for PDs ($p > 0.26$) and PNs ($p > 0.44$). For PDs, we were unable to distinguish between the V and AP directions ($p > 0.59$). HCs had no statistical differences in d_7 signals between ML and V/AP directions ($p > 0.09$). PDs had higher energy for the signals along the V-axis than for signals along the ML-axis ($p < 0.05$). We also observed that signals for all three groups in the 6th decomposition level had higher energy in the V direction than in the ML direction ($p \ll 0.01$). The same results were obtain when we compared signals in the AP and ML directions ($p \ll 0.01$). For HCs in particular, there were no difference between signals in the V and AP directions ($p > 0.45$). For PN subjects, energy in the V direction was higher than in the AP direction ($p \ll 0.01$). Finally the energy was higher in d_5 signals in the ML direction than in the AP direction for PN patients ($p \ll 0.01$) but we were unable to distinguish between signals in the ML and V directions for HCs and PDs ($p > 0.14$) nor between signals in the ML and AP directions for PD subjects ($p > 0.29$).

We found no significant difference between Θ_{ML} and Θ_V for PD and PN subjects after correction ($p > 0.19$), nor between Θ_{ML} and Θ_{AP} for HC and PD subjects ($p > 0.28$) nor between Θ_{AP} and Θ_V for PN subjects ($p > 0.06$).

4.1.3.3 Denoised data The energy repartition for denoised data was similar to the original signal. We still had more than 99% of the energy concentrated in the approximation signal $\Phi_{Va_{10}}$. The energy and the entropy of the signals followed the same trend as the original ones.

When we analyzed the a_{10} signals there was no significantly different energy between signals in the V and AP directions for PD and PN subjects ($p > 0.05$). For healthy subjects we were not able to distinguish between signals in the AP and the ML directions ($p > 0.06$). Similarly for PD subjects, we were not able to distinguish between signals along the V-axis and the ML-axis ($p > 0.05$). The signals in the 8th decomposition level followed the same trend as the corresponding corrected signals while d_7 and d_6 signals followed the same same

trend as the corresponding raw signals. Lastly we analyzed d_5 signals and we noticed for PNs that energy was higher in signals in the ML direction compared to accelerations in the AP direction ($p < 0.04$). This was not case however for PD patients ($p > 0.07$).

The entropy of signals in the ML direction was not significantly different from the one of signals in the AP direction for the PD group ($p > 0.25$). Otherwise the entropy of denoised signals followed the same trend as the raw signals.

4.1.3.4 Corrected and denoised data Similarly to the corrected signals the repartition of the energy was different. In the ML direction, the energy in the approximation signal a_{10} was higher for PD subjects than for HC ones ($p < 0.04$). On the contrary, there was more energy in the d_7 ($p \ll 0.01$) and d_6 ($p < 0.04$) signals for healthy controls than for PD patients. The energy in the d_8 ($p < 0.04$) and d_7 ($p \ll 0.01$) signals was also higher for healthy controls than for PN subjects. Still along the ML-axis, PN patients had higher energy than HCs in the d_5 signal ($p < 0.02$). In the V direction the relative energy of the d_6 signal was lower for PDs than for PNs ($p < 0.01$). In the d_5 signal the opposite was observed ($p < 0.01$). In the AP direction the energy in the d_7 and d_6 signals was higher for the HC group than for the PD ($p < 0.04$) and PN groups ($p < 0.02$). Also, the energy in the d_5 signal was higher for PD subjects compared to PNs ($p < 0.03$).

No difference between groups were observed when we analyzed entropies in every direction ($p > 0.18$). We did not observed differences between anatomical directions neither for PDs and PNs ($p > 0.15$). Only signals from healthy controls had a larger entropy along the ML-axis ($p < 0.05$) and AP-axis ($p < 0.04$) compared to the V-axis.

The energy in the a_{10} signals was similar to the energy in signals after correction. However for PN subjects, we observed that signals in the V direction contained less energy than signals in the ML direction ($p < 0.04$). For the same group of subjects, the energy along the V-axis was also lower than energy in signals along the AP-axis ($p < 0.05$). In the d_7 signals PD subjects had higher energy in the V direction than in the ML ($p < 0.03$) and AP directions ($p < 0.04$). Results for the d_8, d_6 and d_5 signals were the same as the corresponding signals after the correction step. The same trend as for corrected signals was observed when we examined the wavelet entropy differences, except that Θ_{AP} and Θ_V were not statistically different for PDs ($p > 0.15$).

4.1.3.5 Denoised and corrected data The results were very similar to the ones we found in the previous step. Energy in signals from PD subjects was higher than in signals measured on HCs in the V direction ($p < 0.05$).

The same trend was observed compared to accelerations in the previous step except that we did not observe a significant difference of energy between signals in the AP and V directions for PN subjects in the a_{10} approximation signal ($p > 0.05$) nor for PD subjects in the d_7 detail signal ($p > 0.07$). The entropy after the denoised-corrected step followed the same trend as the previous step.

4.2 DISCUSSION ON THE EFFECTS OF PRE-PROCESSING

We successfully extracted features in time, frequency and time-frequency domains. The presented results led us to believe that applying tilt correction and analyzing the corrected data could lead to further discrimination between the three groups.

In the time domain, by applying the tilt correction, we were able to distinguish between healthy controls and subjects with Parkinson's disease and peripheral neuropathy. Specifically, we observed greater skewness for subjects suffering from peripheral neuropathy than for healthy controls in the medio-lateral direction. Nevertheless, no difference between participants having Parkinson's disease and peripheral neuropathy could be observed using this

feature. Concerning harmonic ratios, using the original data the only group differences found were between healthy controls and persons with Parkinson's disease, where controls exhibited greater walking symmetry in all directions of motion. The tilt correction led to further discrimination between the groups and showed that participants with peripheral neuropathy had a greater symmetry than those with Parkinson's disease, whereas healthy controls had a greater symmetry than subjects with peripheral neuropathy. Also, the tilt correction showed that every group had a harmonic ratio higher in the vertical than in the anterior-posterior direction.

In the frequency domain and after tilt correction was applied, peak frequencies in the medio-lateral direction and the spectral centroids in the anterior-posterior direction allowed to distinguish between controls and clinical groups. Also, the bandwidth of signals for subjects with peripheral neuropathy was greater than for healthy controls in the anterior-posterior direction after applying tilt correction.

Time-frequency features were the most difficult to analyze. An obvious observation is that the application of tilt correction changed the energy repartition for every group especially in the vertical direction. The energy was transferred from the approximation signal representing low frequencies to the first six detail signals representing higher frequencies. However it was difficult to distinguish between groups using the features in this domain.

Denoising had practically no effect on the calculated characteristics since, as shown in Figure 9, the signals had a low level of noise. Finally, when applying both correction and denoising we observed that most of the time our corrected and denoised results were the accumulation of the results found when we applied the preprocesses separately.

4.3 RESULTS FROM THE SECOND STUDY

4.3.1 Stride-interval-based features

We noticed no statistical group differences when we used maximum Lyapunov exponents as features ($p > 0.05$). Within group comparisons showed that HCs had a higher Lyapunov exponent in the ML direction during NT in comparison to DT1 ($p < 0.05$). PNs and PDs had a higher Lyapunov exponent in the medio-lateral direction during NT in comparison to DT 2 ($p < 0.01$).

During NT, PNs had a higher harmonic ratio than PDs in the vertical direction ($p < 0.05$). During all tasks, HCs had a higher harmonic ratio than PDs in the V and AP directions ($p < 0.02$) and PNs in the AP direction ($p \ll 0.01$). HCs and PNs had a higher harmonic ratio in all three anatomical directions when performing NT in comparison to DT1 ($p < 0.01$) and DT2 ($p < 0.02$). PDs had a higher harmonic ratio in all three anatomical directions when performing NT in comparison to DT2 ($p < 0.04$). They also had a higher harmonic ratios in the V and AP directions during NT in comparison to DT1 ($p < 0.01$).

There were no group differences using the mean stride interval ($p > 0.33$). HCs had a higher MSI when performing DT2 in comparison to NT ($p < 0.01$).

No group differences were observed using the coefficient of variation for the stride intervals ($p > 0.19$). HCs had a higher CV when performing NT ($p \ll 0.01$) and DT1 ($p < 0.03$) in comparison to DT2. PNs had a higher CV when performing NT in comparison to DT2 ($p < 0.05$).

4.3.2 Statistical features

There were no statistical group differences using standard deviation ($p > 0.11$). All three groups had a higher standard deviation in the V direction when performing NT in comparison to DT1 ($p < 0.01$). PNs also had higher values of standard deviation in the ML direction during N compared to DT1 ($p < 0.04$) and in the V direction during N compared to DT2 ($p \ll 0.01$).

During NT, we observed that PNs had a higher skewness than HCs in the ML direction ($p < 0.01$), while HCs had a higher skewness than PDs in the AP direction ($p < 0.05$). HCs also had a higher skewness than PNs in the AP direction ($p < 0.01$) during DT1 and DT2.

Within group comparisons showed that HCs had a higher skewness in the ML direction when performing DT2 in comparison to NT ($p < 0.04$). All three groups had a higher skewness in the V direction when performing NT in comparison to DT1 ($p < 0.01$) and DT2 ($p < 0.01$). PNs also had a higher skewness in the AP direction when performing NT in comparison to DT1 ($p < 0.01$) and DT2 ($p < 0.01$). During DT1 and DT2, we observed that PNs had a higher kurtosis than HCs in the AP direction ($p \ll 0.01$).

In within group comparisons, HCs and PNs had a higher kurtosis in the ML direction when performing DT1 ($p \ll 0.01$) and DT2 ($p < 0.01$) in comparison to NT, while PDs had a higher kurtosis in the ML direction only when performing the DT1 task in comparison to NT ($p < 0.04$). HCs and PDs had a higher kurtosis in the AP direction when performing DT1 ($p \ll 0.01$) and DT2 ($p < 0.01$) in comparison to NT.

We saw no group differences using cross-correlation ($p > 0.43$) and no task differences ($p > 0.12$).

4.3.3   Information-theoretic features

During NT and DT1, HCs had a higher LZ complexity than PDs and PNs in the ML direction ($p < 0.01$) and the AP direction ($p < 0.02$). During DT2, HCs had a higher LZ complexity than PDs and PNs in the AP direction ($p < 0.02$) and a higher LZ complexity than PNs in the ML direction ($p < 0.01$).

Within group comparisons showed that HCs and PDs had a higher LZ complexity in the V direction when performing DT1 in comparison to NT ($p < 0.02$).

During DT1, we observed that PDs had a higher entropy rate than HCs in every anatomical direction ($p < 0.03$). PNs had a higher entropy rate than HCs in the ML direction only ($p < 0.01$).

Within group comparisons showed that all groups had a higher entropy rate in all anatomical directions ($p < 0.01$) during NT in comparison to DT1. When they performed NT, HCs

($p < 0.04$) and PDs ($p < 0.02$) had a higher entropy rate in the V direction in comparison to DT2. PNs had a higher entropy rate in the AP direction during NT compared to DT2 ($p < 0.02$) while PDs had a higher entropy rate in the ML direction ($p < 0.01$).

During DT1, PDs had a higher synchronization index between the ML and AP directions than HCs ($p < 0.04$).

Within group comparisons showed that HCs had a higher synchronization index between the ML and AP directions when performing NT in comparison to DT1 ($p < 0.01$).

4.3.4 Frequency features

During DT2, we observed that the PN group had a higher peak frequency than HCs in the AP direction ($p < 0.03$).

During group comparisons, HCs had a higher peak frequency in the V and AP directions when performing NT compared to the DT2 task ($p \ll 0.01$).

PNs had a higher centroid than HCs ($p \ll 0.01$) and PDs ($p < 0.03$) in the AP direction during DT1 and higher centroids than HCs during DT2 ($p \ll 0.01$).

Within group comparisons revealed that all three groups had a higher centroid in the ML and AP directions when performing DT1 ($p < 0.01$) and DT2 ($p < 0.01$) in comparison to NT. HCs and PNs also had a higher centroid in the V direction during DT1 in comparison to NT ($p < 0.04$), with PNs also maintaining this relationship even when comparing DT2 and NT($p < 0.01$).

During NT, PDs had a higher bandwidth than HCs in the ML direction ($p < 0.03$) and the AP direction ($p < 0.01$), while PNs had a higher bandwidth than HCs in the AP direction ($p < 0.03$). During DT1, PNs and PDs had a higher bandwidth than HCs in the AP direction ($p \ll 0.01$), while PNs also had a higher bandwidth than HCs in the ML direction as well ($p < 0.01$). During DT2, PNs had a higher bandwidth than HCs in the ML direction ($p < 0.02$) and the AP direction ($p \ll 0.01$). Moreover during the same task, we observed that the PD group had a higher bandwidth than HCs in the AP direction ($p < 0.01$).

Within group comparisons revealed that all groups had a higher bandwidth in all anatomical directions when performing DT1 ($p < 0.01$) and DT2 ($p < 0.01$) in comparison to NT.

4.3.5 Time-frequency features

In the time-frequency analysis, we discarded energy levels which contained less than 5% of energy. In our results, these were the d_{10}, d_9 and d_4 to d_1 decomposition levels.

During NT, we observed a higher relative energy for PDs in comparison to HCs in the ML direction ($p < 0.03$) while there was a higher energy for PNs in comparison to HCs in the AP direction ($p < 0.04$). During DT2, PNs had a higher energy than HCs in the ML direction ($p < 0.05$).

We observed that HCs had a higher energy than PNs in the ML direction ($p < 0.01$).

Within group comparisons showed that HCs had a higher energy in all anatomical directions when performing NT in comparison to DT1 ($p < 0.01$) and DT2 ($p < 0.01$). PNs had a higher energy in the V direction when performing NT in comparison to DT1 ($p < 0.01$) and DT2 ($p < 0.01$). PNs also had a higher energy in the AP direction when performing NT compared to DT1 ($p < 0.02$).

During NT and DT2, HCs had a higher energy than PDs and PNs in the ML ($p < 0.01$) and the AP directions ($p < 0.01$). During DT1, HCs had a higher energy than PNs and PDs in the ML direction ($p < 0.04$) and the AP direction ($p \ll 0.01$).

Within group comparisons showed that HCs had a higher energy in the ML and AP directions when performing NT compared to DT1 ($p < 0.01$) and DT2 ($p < 0.01$). All three groups had a higher energy in the V direction when performing NT compared to DT1 only ($p < 0.02$), and PDs and PNs also had a higher energy in the AP direction ($p < 0.01$). PNs had a higher energy in the ML direction when performing NT compared to DT2 ($p < 0.04$).

During NT, HCs had a higher energy than PDs in all anatomical directions ($p < 0.03$) and a higher energy than PNs in the AP direction ($p < 0.01$). PNs also had a higher energy than PDs in the V direction ($p \ll 0.01$).

Within group comparisons showed that HCs had a higher energy in the AP direction when performing NT compared to DT2 ($p < 0.03$) while PDs had a higher energy in the the same direction when performing NT in comparison to DT1 ($p < 0.01$).

During NT, PNs had a higher energy than HCs in the ML direction ($p \ll 0.01$). Furthermore, PDs had a higher energy than PNs in the V direction ($p < 0.02$) and the AP direction ($p < 0.01$). During DT1, HCs ($p < 0.01$) and PDs ($p < 0.05$) had a higher energy than PNs in the AP direction.

Within group comparisons showed that HCs and PDs had a higher energy in the ML direction when performing NT compared to DT1 ($p < 0.03$). On the contrary, HCs had a higher energy in the V direction when performing DT1 compared to the NT ($p \ll 0.01$). PNs had a higher energy in the V direction when performing DT1 ($p < 0.01$) and DT2 ($p \ll 0.01$) compared to NT. PDs also had a higher energy in the AP direction when performing NT compared to the DT2 task ($p < 0.03$).

No group differences were noticed when we used wavelet entropy ($p > 0.05$).

Within group comparisons revealed that PN participants had a higher entropy in the V direction ($p < 0.04$) and the AP direction ($p < 0.03$) when performing DT2 in comparison to NT. PDs had a higher entropy in the ML direction when performing NT compared to DT1 ($p < 0.05$).

4.3.6 Summary

Tables 6 and 7 summarize our results.

4.4 DISCUSSION ON THE EFFECTS OF DUAL-TASK WALKING

In this study, we considered signal features from stride interval time series and gait accelerometry signals during walks that involved walking at normal speed and dual-task walking.

Table 6 summarized group differences for different tasks. Regardless of walking conditions, the maximum Lyapunov exponents, mean stride intervals, coefficients of variation for stride intervals, standard deviations, cross-correlations and wavelet entropies did not distinguish among groups. The results thus suggest that these features are not adequate to reveal pathologies.

Group differences, however, were observed when using the rest of the feature set. In this set, several features showed almost the same group differences for each task. This was the case with the Lempel-Ziv complexity, harmonic ratios, bandwidth of accelerations and the d_7 level of wavelet decomposition, which were therefore unaffected by dual-tasking. HCs had a higher harmonic ratio than PDs in the V and AP directions, indicating that participants with Parkinson's disease had a less symmetric walk than controls. Similarly, HCs had a more symmetric walk than PNs as a higher harmonic ratio in the AP direction for controls indicated.

Other features highlighted differences for specific tasks. In the case of skewness, which is a measure of the symmetry of a distribution, this feature allowed us to distinguish between controls and clinical groups during NT. Furthermore, we observed a statistical difference between controls and subjects with peripheral neuropathy during the DT1 and DT2 tasks. The differences we observed were visible when analyzing accelerations in the AP and ML directions during the normal task, but they were visible in the AP direction only during the other tasks.

Table 6: Within task comparisons.

Legend: ▲: ML / ■: V / ◆: AP / ★: ML,V / †:ML,AP / ‡:V,AP

		λ_L	HIR	MSI	CV	σ	ξ	γ	η	LZC	ρ	Λ	f_p	f_c	BW	$\Phi_{a_{10}}$	Φ_{d_8}	Φ_{d_7}	Φ_{d_6}	Φ_{d_5}	Θ
NT	$HC > PD$	-	■,◆	-	-	-	◆	-	-	▲,◆	-	-	-	-	-	-	-	▲,◆	▲,◆,	-	-
	$HC > PN$	-	◆	-	-	-	-	-	-	▲,◆	-	-	-	-	-	-	-	▲,◆	◆	▲	-
	$PN > HC$	-	-	-	-	-	▲	-	-	-	-	-	-	-	◆	◆	▲	-	-	-	-
	$PN > PD$	-	■	-	-	-	-	-	-	-	-	-	-	-	-	-	-	-	■	-	-
	$PD > PN$	-	-	-	-	-	-	-	-	-	-	-	-	-	-	-	-	-	-	■,◆	-
	$PD > HC$	-	-	-	-	-	-	-	-	-	-	-	-	-	▲,◆	▲	-	-	-	-	-
DT 1	$HC > PD$	-	■,◆	-	-	-	◆	-	-	▲,◆	-	-	-	-	-	-	-	▲,◆	-	-	-
	$HC > PN$	-	◆	-	-	-	-	◆	-	▲,◆	-	-	-	-	-	-	-	▲,◆	-	◆	-
	$PN > HC$	-	-	-	-	-	-	-	-	-	▲	-	-	◆	▲,◆	-	-	-	-	-	-
	$PN > PD$	-	-	-	-	-	-	-	-	-	-	-	-	◆	-	-	-	-	-	-	-
	$PD > PN$	-	-	-	-	-	-	-	-	-	-	-	-	-	-	-	-	-	-	◆	-
	$PD > HC$	-	-	-	-	-	-	-	-	◆	▲,■,◆	†	-	-	◆	-	-	-	-	-	-
DT 2	$HC > PD$	-	■,◆	-	-	-	◆	-	-	◆	-	-	-	-	-	-	-	▲,◆	-	-	-
	$HC > PN$	-	◆	-	-	-	-	◆	-	▲,◆	-	-	-	-	-	-	-	▲,◆	-	-	-
	$PN > HC$	-	-	-	-	-	-	-	-	-	-	-	◆	◆	▲,◆	▲	-	-	-	-	-
	$PN > PD$	-	-	-	-	-	-	-	-	-	-	-	-	-	-	-	-	-	-	-	-
	$PD > PN$	-	-	-	-	-	-	-	-	-	-	-	-	-	-	-	-	-	-	-	-
	$PD > HC$	-	-	-	-	-	-	-	-	-	-	-	-	-	◆	-	-	-	-	-	-

49

Table 7: Within group comparisons.

Legend: ◀: ML / ■: V / ◆: AP / ★: ML,V / †:ML,AP / ‡:V,AP / •: Significant difference

		λ_L	HR	MSI	CV	σ	ξ	γ	η	LZC	ρ	Λ	f_p	f_c	BW	$\Phi_{a_{10}}$	Φ_{d_8}	Φ_{d_7}	Φ_{d_6}	Φ_{d_5}	Θ
HC	$NT > DT1$	◀	◀,■,◆	-	-	■	■	-	-	-	◀,■,◆	†	-	-	-	-	◀,■,◆	◀,■,◆	-	◀	-
	$NT > DT2$	-	◀,■,◆	-	•	-	■	-	-	-	■	-	■,◆	-	-	-	◀,■,◆	◀,◆	◆	■	-
	$DT1 > NT$	-	-	-	-	-	-	◀,◆	-	■	-	-	-	◀,■,◆	◀,■,◆	-	-	-	-	-	-
	$DT1 > DT2$	-	-	-	•	-	-	-	-	-	-	-	-	-	-	-	-	-	-	-	-
	$DT2 > NT$	-	-	•	•	-	◀	◀,◆	-	-	-	-	-	◀,◆	◀,■,◆	-	-	-	-	-	-
	$DT2 > DT1$	-	-	-	-	-	-	-	-	-	-	-	-	-	-	-	-	-	-	-	-
PN	$NT > DT1$	-	◀,■,◆	-	-	◀,■	◀,■	-	-	-	◀,■,◆	-	-	◀,■,◆	◀,■,◆	-	◆	◆	-	-	-
	$NT > DT2$	◀	◀,■,◆	-	-	◀,■	◀,■	-	-	-	◆	-	-	-	-	-	■	◀	-	■	-
	$DT1 > NT$	-	-	-	•	-	-	◀	-	-	-	-	-	◀,■,◆	◀,■,◆	-	-	-	-	■	-
	$DT1 > DT2$	-	-	-	-	-	-	-	-	-	-	-	-	-	-	-	-	-	-	-	-
	$DT2 > NT$	-	-	-	-	-	-	◀	-	-	-	-	-	◀,■,◆	◀,■,◆	-	-	-	-	■	■,◆
	$DT2 > DT1$	-	-	-	-	-	-	-	-	-	-	-	-	-	-	-	-	-	-	-	-
PD	$NT > DT1$	-	■,◆	-	-	■	■	-	-	-	◀,■,◆	-	-	-	-	-	■	◆	◆	◀	◀
	$NT > DT2$	◀	◀,■,◆	-	-	-	■	-	-	-	◀,■	-	-	-	-	-	-	-	-	◆	-
	$DT1 > NT$	-	-	-	-	-	-	◀,◆	-	■	-	-	-	◀,◆	◀,■,◆	-	-	-	-	-	-
	$DT1 > DT2$	-	-	-	-	-	-	-	-	-	-	-	-	-	-	-	-	-	-	-	-
	$DT2 > NT$	-	-	-	-	-	-	◆	-	-	-	-	-	◀,◆	◀,■,◆	-	-	-	-	-	-
	$DT2 > DT1$	-	-	-	-	-	-	-	-	-	-	-	-	-	-	-	-	-	-	-	-

50

Interestingly, depending on the task performed, differences concerning controls and PN subjects had a different meaning, and were observed in different anatomical directions. Indeed, PNs had a higher skewness than controls in the ML direction during the normal task. However, during the other tasks, controls had a higher skewness than PN participants in the AP direction. Thus, the tasks performed had an impact on the feature, and the changes in this feature should be interpreted cautiously.

Kurtosis, a measure of "peakedness" of a distribution, did not allow us to discriminate among groups during the normal task. On the contrary, during the DT1 and DT2 tasks, the kurtosis of accelerations in the AP direction were different between PNs and HCs.

PNs had higher spectral centroids than HCs during DT1 and DT2. Spectral centroids divide the power spectrum into two equal parts. An increased spectral centroid value means that more high-frequency components are present in the spectrum of a signal. This result was anticipated, since PNs generally have a less stable walk due to the loss of sensitivity in the extremities. More oscillations were therefore captured by the accelerometer. During DT1, our results suggest the effects of this instability were stronger than the tremor of PDs, since PNs had statistically higher spectral centroids than PDs.

Group differences for entropy rate and synchronization index were noticed during DT1 specifically. The entropy rate measures the regularity of patterns in a signal, and our results showed an increased entropy rate for PDs compared to controls in all anatomical directions. Increased regularity in biomedical signals has been associated with pathologies in previous studies [81].

Relative energy in the d_6 level of decomposition showed group differences during the normal task, but not during the other tasks. Therefore, dual-tasking also had an impact on group comparisons for these features.

In conclusion, three features stood out for the constancy in the differences they showed: the Lempel-Ziv complexity, the bandwidth of accelerations and harmonic ratios. Other features were affected by the task that was performed.

Table 7 summarizes task differences for the three groups. Across all groups of subjects, we did not notice differences using cross-correlation or the relative energy in the a_{10} level of decomposition. With the rest of the features, practically the same task differences were observed for each group.

We analyzed the accelerations in the ML direction and noticed that the maximum Lyapunov exponent was higher during the normal task than during the other tasks for all groups. This result indicates that subjects were less stable during the normal task compared to the other tasks. It is possible that subjects became habituated to the task they performed and gained assurance, hence the higher instability during the normal task, which corresponds to the beginning of the experiment. For HCs, the coefficient of variation of stride intervals was higher during the normal task compared with the DT1 task, which correlates with a higher instability. However, no differences could be seen for the other tasks. Similarly, PNs had a higher coefficient of variation during the normal task compared with the DT2 task. No such differences were visible for PDs.

HCs also walked with a higher mean stride interval during DT2 compared with the normal task, but this was not the case for the other groups. All groups had a more symmetric walk during the normal task compared with the other tasks. This result was visible when analyzing the accelerations in every anatomical direction, and it shows a decrease in performance while the subjects were performing another task while walking.

5.0 CONCLUSIONS AND FUTURE WORK

5.1 CONCLUSIONS

In the first study, we pre-processed gait accelerometry signals using different techniques in order to understand the impact on the extracted signal features in time, frequency and time-frequency domains. Specifically, we examined the effects of tilt correction and denoising as well as their combined effects. The results have shown that pre-processing may yield additional discrimination between the considered groups. Hence, future studies should consider pre-processing gait accelerometry signals before extracting any features.

It is of primary importance that researchers use a common base of signal features when performing gait analysis. In the second study we extracted time, frequency, time-frequency and information-theoretic features from stride intervals and accelerometry signals, and we analyzed the impact of dual-task walking on them. We found that the differences between healthy controls and clinical groups revealed by Lempel-Ziv complexity, bandwidth of signals and harmonic ratios were not impacted by the fact that another task was performed, but other features were impacted. We also found that all subjects had lower harmonic ratios when dual-task walking, which shows a degradation in performance. Future studies should confirm if this is an age-related issue. Future publications should also continue using a wide base of features in order to choose relevant ones and use them in a clinical context.

5.2 FUTURE WORK

In the future, studies about quiet standing and dynamic gait analysis should be compared so as to confirm and eventually find new conclusions about stability of subjects. Moreover, our studies have focused on accelerations of the trunk during walking, but the latter involves interactions with different systems. Monitoring these interactions (e.g. measuring oxygen consumption) may be useful to obtain more insights about the mechanisms of gait and the different strategies used to minimize the energy consumed during a walk.

BIBLIOGRAPHY

[1] R. Baker, "The history of gait analysis before the advent of modern computers," *Gait & Posture*, vol. 26, no. 3, pp. 331–342, 2007.

[2] M. Whittle, "Clinical gait analysis: A review," *Human Movement Science*, vol. 15, pp. 369–387, 1996.

[3] D. H. Sutherland, "The evolution of clinical gait analysis part l: kinesiological EMG," *Gait & Posture*, vol. 14, no. 1, pp. 61–70, 2001.

[4] A. Wing and P. Beek, "Motion analysis: A joint centenary," *Human Movement Science*, vol. 23, no. 5, pp. iii–iv, 2004.

[5] S. R. Simon, "Quantification of human motion: gait analysis - benefits and limitations to its application to clinical problems," *Journal of Biomechanics*, vol. 37, no. 12, pp. 1869–1880, 2004.

[6] W. Tao, T. Liu, R. Zheng, and H. Feng, "Gait analysis using wearable sensors," *Sensors*, vol. 12, no. 2, pp. 2255–2283, 2012.

[7] D. A. Winter, "Human balance and posture control during standing and walking," *Gait & Posture*, vol. 3, no. 4, pp. 193–214, 1995.

[8] D. Knudson, *Fundamentals of Biomechanics*. Springer, 2nd ed., 2007.

[9] C. Kirtley, *Clinical Gait Analysis - Theory and Practice*. Elsevier, 2006.

[10] C. T. Farley and D. P. Ferris, "Biomechanics of Walking and Running: Center of Mass Movements to Muscle Action," *Exercise and Sport Sciences Reviews*, vol. 26, pp. 253–286, 1998.

[11] R. J. Peterka, "Sensorimotor integration in human postural control," *Journal of Neurophysiology*, vol. 88, no. 3, pp. 1097–1118, 2002.

[12] W. Warren, B. Kay, W. Zosh, A. P. Duchon, and S. Sahuc, "Optic flow is used to control human walking," *Nature Neuroscience*, vol. 4, no. 2, pp. 213–217, 2001.

[13] F. B. Horak, "Postural orientation and equilibrium: what do we need to know about neural control of balance to prevent falls?," *Age and Ageing*, vol. 35-S2, pp. ii7–ii11, 2006.

[14] D. H. Sutherland, "The evolution of clinical gait analysis part III - kinetics and energy assessment," *Gait & Posture*, vol. 21, no. 4, pp. 447–461, 2005.

[15] R. H. Rozendal, "Clinical gait analysis: Problems and solutions?," *Human Movement Science*, vol. 10, pp. 555–564, 1991.

[16] J. Baumann, "Requirements of clinical gait analysis," *Human Movement Science*, vol. 10, no. 5, pp. 535–542, 1991.

[17] V. P. Panzer, S. Bandinelli, and M. Hallett, "Biomechanical assessment of quiet standing and changes associated with aging," *Archives of Physical Medicine and Rehabilitation*, vol. 76, no. 2, pp. 151–157, 1995.

[18] E. van Wegen, R. van Emmerik, and G. Riccio, "Postural orientation: Age-related changes in variability and time-to-boundary," *Human Movement Science*, vol. 21, no. 1, pp. 61–84, 2002.

[19] B. R. Bloem, J. M. Hausdorff, J. E. Visser, and N. Giladi, "Falls and freezing of gait in Parkinson's disease: a review of two interconnected, episodic phenomena.," *Movement Disorders*, vol. 19, no. 8, pp. 871–84, 2004.

[20] M. Schenkman, M. Morey, and M. Kuchibhatla, "Spinal Flexibility and Balance Control Among Community-Dwelling Adults With and Without Parkinson's Disease," *Journal of Gerontology: Medical Sciences*, vol. 55A, no. 8, pp. M441–M445, 2000.

[21] J. D. Schaafsma, N. Giladi, Y. Balash, A. L. Bartels, T. Gurevich, and J. M. Hausdorff, "Gait dynamics in Parkinson's disease: relationship to Parkinsonian features, falls and response to levodopa," *Journal of the Neurological Sciences*, vol. 212, no. 1, pp. 47–53, 2003.

[22] M. J. Mueller, S. D. Minor, S. A. Sahrmann, J. A. Schaaf, and M. J. Strube, "Differences in the Gait Characteristics of Patients With Diabetes and Peripheral Neuropathy Compared With Aged-Matched Controls," *Physical Therapy*, vol. 74, pp. 299–308, 1994.

[23] G. G. Simoneau, J. S. Ulbrecht, J. A. Derr, M. B. Becker, and P. R. Cavanagh, "Postural Instability in Patients With Diabetic Sensory Neuropathy," *Diabetes Care*, vol. 17, no. 12, pp. 1411–1421, 1994.

[24] J. M. Hausdorff, D. A. Rios, and H. K. Edelberg, "Gait variability and fall risk in community-living older adults: a 1-year prospective study," *Archives of Physical Medicine and Rehabilitation*, vol. 82, no. 8, pp. 1050–1056, 2001.

[25] M. C. Hornbrook, V. J. Stevens, D. J. Wingfield, J. F. Hollis, M. R. Greenlick, and M. G. Ory, "Preventing falls among community-dwelling older persons: results from a randomized trial," *The Gerontologist*, vol. 34, pp. 16–23, 1994.

[26] M. K. Karlsson, T. Vonschewelov, C. Karlsson, M. Cöster, and B. E. Rosengen, "Prevention of falls in the elderly: a review," *Scandinavian Journal of Public Health*, vol. 41, no. 5, pp. 442–54, 2013.

[27] A. Patla, J. Frank, and D. Winter, "Assessment of balance control in the elderly: major issues," *Physiotherapy Canada*, vol. 42, no. 2, pp. 89–97, 1990.

[28] W. Zijlstra and K. Aminian, "Mobility assessment in older people: new possibilities and challenges," *European Journal of Ageing*, vol. 4, pp. 3–12, Feb. 2007.

[29] R. Moe-Nilssen, "A new method for evaluating motor control in gait under real-life environmental conditions. Part 2: Gait analysis," *Clinical Biomechanics*, vol. 13, pp. 328–335, 1998.

[30] M. Woollacott and A. Shumway-Cook, "Attention and the control of posture and gait: a review of an emerging area of research," *Gait & Posture*, vol. 16, no. 1, pp. 1–14, 2002.

[31] R. Beurskens and O. Bock, "Age-related deficits of dual-task walking: a review," *Neural Plasticity*, vol. 2012, p. 131608, 2012.

[32] M. Gu, A. Schultz, N. Shepard, and N. Alexander, "Postural control in young and elderly adults when stance is perturbed: dynamics," *Journal of Biomechanics*, vol. 29, no. 3, pp. 319–329, 1996.

[33] R. Moe-Nilssen and J. Helbostad, "Trunk accelerometry as a measure of balance control during quiet standing," *Gait & Posture*, vol. 16, pp. 60–68, 2002.

[34] R. Mayagoitia, J. Lötters, P. Veltink, and H. Hermens, "Standing balance evaluation using a triaxial accelerometer," *Gait & Posture*, vol. 16, pp. 55–59, 2002.

[35] M. K. Viitasalo, V. Kampman, K. A. Sotaniemi, S. Leppävuori, V. V. Myllylä, and J. T. Korpelainen, "Analysis of sway in Parkinson's disease using a new inclinometry-based method," *Movement Disorders*, vol. 17, no. 4, pp. 663–669, 2002.

[36] J. B. Geursen, D. Altena, C. H. Massen, and M. Verduin, "A model of the standing man for the description of his dynamic behaviour," *Agressologie*, vol. 17, pp. 63–69, 1976.

[37] B. J. Benda, P. O. Riley, and D. E. Krebs, "Biomechanical relationship between center of gravity and center of pressure during standing," *IEEE Transactions on Rehabilitation Engineering*, vol. 2, no. 1, pp. 3–10, 1994.

[38] W. P. Berg, H. M. Alessio, E. M. Mills, and C. Tong, "Circumstances and consequences of falls in independent community-dwelling older adults," *Age and Ageing*, vol. 26, no. 4, pp. 261–268, 1997.

[39] N. Niino, S. Tsuzuku, F. Ando, and H. Shimokata, "Frequencies and circumstances of falls in the National Institute for Longevity Sciences, Longitudinal Study of Aging (NILS-LSA)," *Journal of Epidemiology / Japan Epidemiological Association*, vol. 10, pp. S90–S94, 2000.

[40] L. A. Talbot, R. J. Musiol, E. K. Witham, and E. J. Metter, "Falls in young, middle-aged and older community dwelling adults: perceived cause, environmental factors and injury," *BMC Public Health*, vol. 5, no. 1, p. 86, 2005.

[41] M. Ferdjallah, G. F. Harris, P. Smith, and J. J. Wertsch, "Analysis of postural control synergies during quiet standing in healthy children and children with cerebral palsy," *Clinical Biomechanics*, vol. 17, no. 3, pp. 203–210, 2002.

[42] H. G. Kang and J. B. Dingwell, "A direct comparison of local dynamic stability during unperturbed standing and walking," *Experimental Brain Research*, vol. 172, no. 1, pp. 35–48, 2006.

[43] H. B. Menz, S. R. Lord, and R. C. Fitzpatrick, "Acceleration patterns of the head and pelvis when walking on level and irregular surfaces," *Gait & Posture*, vol. 18, no. 1, pp. 35–46, 2003.

[44] J. B. Saunders, V. T. Inman, and H. D. Eberhart, "The major determinants in normal and pathological gait," *The Journal of Bone and Joint Surgery*, vol. 35-A, no. 3, pp. 543–558, 1953.

[45] J. J. Kavanagh and H. B. Menz, "Accelerometry: a technique for quantifying movement patterns during walking," *Gait & Posture*, vol. 28, no. 1, pp. 1–15, 2008.

[46] K. Aminian and B. Najafi, "Capturing human motion using body-fixed sensors: outdoor measurement and clinical applications," *Computer Animation and Virtual Worlds*, vol. 15, no. 2, pp. 79–94, 2004.

[47] T. B. Moeslund and E. Granum, "A Survey of Computer Vision-Based Human Motion Capture," *Computer Vision and Image Understanding*, vol. 81, no. 3, pp. 231–268, 2001.

[48] T. B. Moeslund, A. Hilton, V. Krüger, P. Fua, and R. Ronfard, "A survey of advances in vision-based human motion capture and analysis," *Computer Vision and Image Understanding*, vol. 104, no. 2, pp. 90–126, 2006.

[49] "Vicon Motion Systems Ltd.," 2013.

[50] "Natural Point, Inc.," 2013.

[51] N. Fusco and A. Crétual, "Instantaneous treadmill speed determination using subject's kinematic data.," *Gait & Posture*, vol. 28, no. 4, pp. 663–7, 2008.

[52] R. Moe-Nilssen, "A new method for evaluating motor control in gait under real-life environmental conditions. Part 1: The instrument," *Clinical Biomechanics*, vol. 13, pp. 320–327, 1998.

[53] G. Smidt, J. Arora, and R. Johnston, "Accelerographic analysis of several types of walking," *American Journal of Physical Medicine*, vol. 50, no. 6, pp. 285–300, 1971.

[54] D. Donoho, "De-noising by soft-thresholding," *IEEE Transactions on Information Theory*, vol. 41, no. 3, pp. 613–627, 1995.

[55] S. Stanković, I. Orović, and E. Sejdić, *Multimedia Signals and Systems.* Springer US, 2012.

[56] E. Sejdić, I. Djurović, and J. Jiang, "Time-frequency feature representation using energy concentration: An overview of recent advances," *Digital Signal Processing*, vol. 19, no. 1, pp. 153–183, 2009.

[57] J. Lee, E. Sejdić, C. M. Steele, and T. Chau, "Effects of liquid stimuli on dual-axis swallowing accelerometry signals in a healthy population," *BioMedical Engineering Online*, vol. 9, p. 7, 2010.

[58] O. Rosso, S. Blanco, and J. Yordanova, "Wavelet entropy: a new tool for analysis of short duration brain electrical signals," *Journal of Neuroscience Methods*, vol. 105, pp. 65–75, 2001.

[59] M. N. Nyan, F. E. H. Tay, K. H. W. Seah, and Y. Y. Sitoh, "Classification of gait patterns in the time-frequency domain," *Journal of Biomechanics*, vol. 39, no. 14, pp. 2647–2656, 2006.

[60] S. Mallat, *A Wavelet tour of signal processing.* Academic Press, 2nd ed., 1999.

[61] A. N. Akansu, M. V. Tazebay, M. J. Medley, and P. K. Das, "Wavelet and Subband Transforms: Fundamentals and Communication Applications," *IEEE Communications Magazine*, pp. 104–115, 1997.

[62] S. Mallat, "A theory for multiresolution signal decomposition: the wavelet representation," *IEEE transactions on Pattern Analysis and Machine Intelligence*, vol. 11, no. 7, pp. 674–693, 1989.

[63] D. Donoho and I. Johnstone, "Adapting to unknown smoothness via wavelet shrinkage," *Journal of the American Statistical Association*, vol. 90, no. 432, pp. 1200–1224, 1995.

[64] K. A. Lowry, A. L. Smiley-Oyen, A. J. Carrel, and J. P. Kerr, "Walking stability using harmonic ratios in Parkinson's disease," *Movement Disorders*, vol. 24, no. 2, pp. 261–267, 2009.

[65] R. Courtemanche, N. Teasdale, P. Boucher, M. Fleury, Y. Lajoie, and C. Bard, "Gait Problems in Diabetic Neuropathic Patients," *Archives of Physical Medicine and Rehabilitation*, vol. 77, no. 9, pp. 849–855, 1996.

[66] J. K. Richardson, S. B. Thies, T. K. DeMott, and J. A. Ashton-Miller, "A comparison of gait characteristics between older women with and without peripheral neuropathy in standard and challenging environments," *Journal of the American Geriatrics Society*, vol. 52, no. 9, pp. 1532–1537, 2004.

[67] E. Sejdić, K. Lowry, J. L. Bellanca, M. S. Redfern, and J. S. Brach, "A Comprehensive Assessment of Gait Accelerometry Signals in Time, Frequency and Time-Frequency Domains," *IEEE Transactions on Neural Systems and Rehabilitation Engineering*, pp. 1–10, 2013.

[68] A. Papoulis, *Probability, Random Variables, and Stochastic Processes.* New York: WCB/McGraw-Hill, 3rd ed., 1991.

[69] E. Sejdić, C. M. Steele, and T. Chau, "The effects of head movement on dual-axis cervical accelerometry signals," *BMC Research Notes*, vol. 3, p. 269, 2010.

[70] J. S. Brach, D. McGurl, D. Wert, J. M. VanSwearingen, S. Perera, R. Cham, and S. Studenski, "Validation of a measure of smoothness of walking," *Journals of Gerontology: Medical Sciences*, vol. 66, no. 1, pp. 136–141, 2011.

[71] J. L. Bellanca, K. A. Lowry, J. M. VanSwearingen, J. S. Brach, and M. S. Redfern, "Harmonic ratios: a quantification of step to step symmetry," *Journal of Biomechanics*, vol. 46, no. 4, pp. 828–831, 2013.

[72] A. Cohen and J. Kovačević, "Wavelets: The mathematical background," *Proceedings of the IEEE*, vol. 84, no. 4, pp. 514–22, 1996.

[73] N. H. Packard, J. P. Crutchfield, J. D. Farmer, and R. S. Shaw, "Geometry from a Time Series," *Physical Review Letters*, vol. 45, no. 9, pp. 712–716, 1980.

[74] M. Rosenstein, J. Collins, and C. Deluca, "A practical method for calculating largest Lyapunov exponents from small data sets," *Physica D: Nonlinear Phenomena*, vol. 65, no. 1-2, pp. 117–134, 1993.

[75] M. Kennel, R. Brown, and H. Abarbanel, "Determining embedding dimension for phase-space reconstruction using a geometrical construction," *Physical Review A*, vol. 45, no. 6, pp. 3403–3411, 1992.

[76] M. D. Chang, E. Sejdić, V. Wright, and T. Chau, "Measures of dynamic stability: Detecting differences between walking overground and on a compliant surface.," *Human movement science*, vol. 29, no. 6, pp. 977–86, 2010.

[77] J. B. Dingwell and L. C. Marin, "Kinematic variability and local dynamic stability of upper body motions when walking at different speeds," *Journal of Biomechanics*, vol. 39, no. 3, pp. 444–452, 2006.

[78] A. Lempel and J. Ziv, "On the complexity of finite sequences," *IEEE Transactions on Information Theory*, vol. IT-22, no. 1, pp. 75–81, 1976.

[79] M. Aboy and R. Hornero, "Interpretation of the Lempel-Ziv complexity measure in the context of biomedical signal analysis," *IEEE Transactions on Biomedical Engineering*, vol. 53, no. 11, pp. 2282–2288, 2006.

[80] R. Ferenets, T. Lipping, A. Anier, V. Jäntti, S. Melto, and S. Hovilehto, "Comparison of entropy and complexity measures for the assessment of depth of sedation," *IEEE Transactions on Biomedical Engineering*, vol. 53, no. 6, pp. 1067–1077, 2006.

[81] A. Porta, G. Baselli, D. Liberati, and N. Montano, "Measuring regularity by means of a corrected conditional entropy in sympathetic outflow," *Biological Cybernetics*, vol. 78, pp. 71–78, 1998.

[82] A. Porta, S. Guzzetti, N. Montano, R. Furlan, M. Pagani, A. Malliani, and S. Cerutti, "Entropy, entropy rate, and pattern classification as tools to typify complexity in short heart period variability series," *IEEE Transactions on Biomedical Engineering*, vol. 48, no. 11, pp. 1282–1291, 2001.

[83] A. Porta, G. Baselli, F. Lombardi, N. Montano, A. Malliani, and S. Cerutti, "Conditional entropy approach for the evaluation of the coupling strength," *Biological Cybernetics*, vol. 81, no. 2, pp. 119–129, 1999.